DIELECTRICS, FERROELECTRICS and MULTIFERROICS

Very useful reading:

1. Ashcroft and Mermin, Solid State Physics

2. M. E. Lines and A. M. Glass, Principles and Applications of Ferroelectrics and Related Materials

3. Karin M. Rabe, Charles H. Ahn, Jean-Marc Triscone Eds., Physics of Ferroelectrics. A Modern Perspective, Topics Appl. Physics 105 (2007)

4. Tokura, Seki and Nagaosa, Rep. Prog. Phys. 77 (2014) 076501

20.05.2015, Ionela Vrejoiu

DIELECTRICS

In contrast to METALS, there are solid materials which have *a region of forbidden energies separating the highest occupied and the lowest unoccupied levels.*

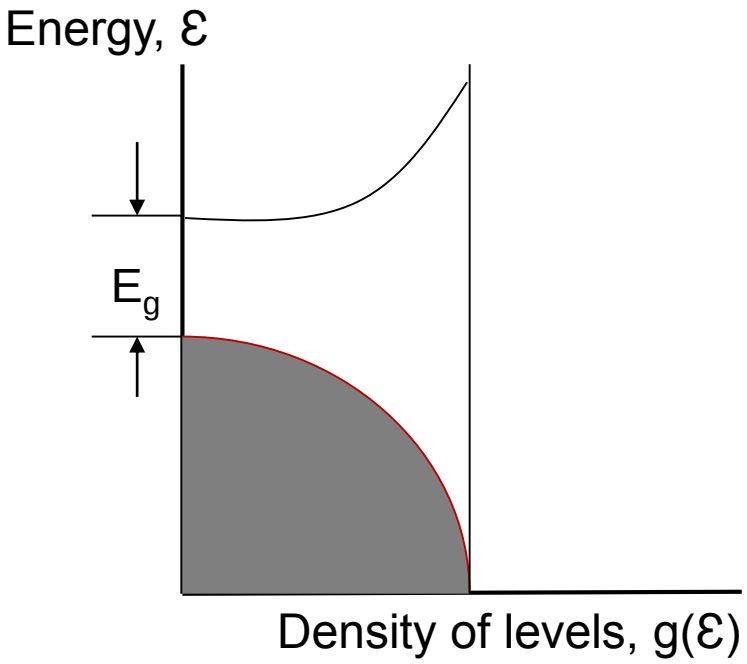

A SOLID WITH AN ENERGY GAP, E_g, WILL BE NONCONDUCTING AT T= 0 K.

T> 0 K: nonvanishing probability that some electrons will be thermally excited across the energy gap into the lowest unoccupied bands, so-called CONDUCTION BANDS, leaving behind unocuppied levels in the highest occupied bands, so-called VALENCE BANDS.

Thermally excited electrons are capable of conduction and *hole*-type conduction can occur in the band out of which the electrons were excited.

Fraction of thermally excited electrons at temperature T: $n_{ex} \sim e^{-Eg/2k_BT}$

Examples: For a material with **E_g= 4 eV**, at T= 300 K- **$n_{ex} \sim 10^{-35}$** - no conduction at RT

E_g= 0.25 eV, at T= 300 K- **$n_{ex} \sim 10^{-2}$**, hence observable conduction can occur at RT

Definitions

SEMICONDUCTORS: solids that are insulators at T= 0 K, but whose energy gap is of such size that THERMAL EXCITATION can lead to observable conductivity at temperatures below their melting point

Examples:

Silicon, Si: E_g= 1.12 eV (at 300 K); 1.17 eV (at 0 K)

Germanium, Ge: E_g= 0.67 eV (at 300 K); 0.75 eV (at 0 K)

Galium arsenide, GaAs: E_g= 1.4 eV (at 300 K)

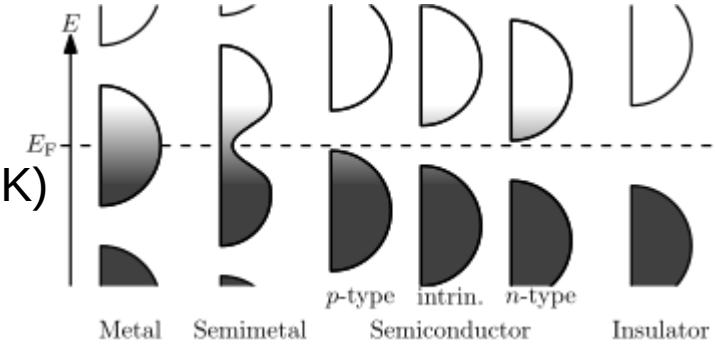

INSULATORS (**DIELECTRICS**):

a semiconductor with the E_g > 2 eV at 300 K

Typical resistivities ρ at 300 K:

Metals: $\rho \approx 10^{-6}\ \Omega$cm

Semiconductors: $\rho \approx 10^{-3} - 10^{9}\ \Omega$cm

Dielectrics (insulators): $\rho \approx 10^{22}\ \Omega$cm

Metals *vs*. Semiconductors: electrical conductivity

For a semiconductor/insulator $n_{ex} \sim e^{-Eg/2k_BT}$

so the conductivity, $\sigma_{semicond}$, is a very rapidly INCREASING function of temperature T.

For a metal: $\sigma_{metal} = (ne^2\tau)/m$

σ_{metal} DECLINES with increasing temperature T;

major T-dependence comes from the relaxation time, τ.

Most striking feature of semiconductors is that, unlike metals, their electrical resistance declines with raising temperature: negative coefficient of resistance.

Important related pehomenon:

PHOTOCONDUCTIVITY of semiconductors and insulators- the increase of conductivity produced by shining (visible) light ($h\nu > 2$ eV) on a semiconductor or insulator.

Dielectric properties of INSULATORS

For insulators: $E_g \geq 2$ eV at 300 K- thermal excitation of free carriers would require temperatures far beyond melting point, T ≥ 30000 K

Examples:

$E_g(SiO_2)$= 9 eV

$E_g(MgO)$= 7.8 eV (optically transparent for wavelenghts 0.3 μm to 7 μm)

$E_g(LaAlO_3)$= 5.2 eV

$E_g(LiNbO_3) \approx$ 4.2 eV

$E_g(BaTiO_3)$= 3.2 eV

CHARGE CARRIERS CANNOT FLOW FREELY IN AN INSULATOR:

applied electric fields of substantial amplitude can penetrate into their interiors and thus affect their internal (atomic) structure.

Important consequences for:

-*Static dielectric response* (static dielectric constant ε_0), which is made use of in capacitors and electronic devices

-*Optical properties of an insulator*: its response to AC electric field associated with electromagnetic radiation, reflected by its frequency dependent dielectric constant $\varepsilon(\omega)$ or equivalently its refractive index $n(\omega) = \sqrt{\varepsilon(\omega)}$.

Macroscopic Maxwell equations of electrostatics

Theory of macroscopic Maxwell equations in a medium is a most valuable tool in dealing with static dielectric constant and optical properties of insulators.

Charge density, $\rho^{micro}(\mathbf{r})$, in an insulator **on atomic scale** is a rapidly varying function of position **r** (reflecting the microscopic atomic structure of the insulator)

On the same atomic scale: electrostatic potential $\Phi^{micro}(\mathbf{r})$ and electric field $\mathbf{E}^{micro}(\mathbf{r})$, related by $\mathbf{E}^{micro}(\mathbf{r}) = -\nabla\cdot\Phi^{micro}(\mathbf{r})$,

have also STRONG and RAPID variations because they are related to charge density via:

$$\nabla\cdot\mathbf{E}^{micro}(\mathbf{r}) = \frac{1}{\varepsilon_0}\rho^{micro}(\mathbf{r})$$

In the conventional MACROSCOPIC electromagnetic theory of insulators, charge density $\rho(\mathbf{r})$, potential $\Phi(\mathbf{r})$, and electric field $\mathbf{E}(\mathbf{r})$ show NO such rapid variations: in an insulator in the absence of an externally applied electric field, $\Phi(\mathbf{r})=0$ or a constant.

$$\nabla\cdot\mathbf{D}(\mathbf{r}) = \rho$$

ρ is the free charge density (due to the excess charges not intrinsic to the medium), that is assumed to be null for an insulator.

Macroscopic Maxwell equations of electrostatics

For an insulator: $\nabla \cdot \mathbf{D}(\mathbf{r}) = 0$

with the **dielectric displacement** $\mathbf{D}(\mathbf{r})$ given by

$$\mathbf{D}(\mathbf{r}) = \varepsilon_0 \mathbf{E}(\mathbf{r}) + \mathbf{P}(\mathbf{r})$$

where $\mathbf{P}(\mathbf{r})$ is the **polarization density**.

Thus: $$\nabla \cdot \mathbf{E}(\mathbf{r}) = -\frac{1}{\varepsilon_0} \nabla \cdot \mathbf{P}(\mathbf{r})$$

$\mathbf{P}(\mathbf{r})$ is generally a very slowly varying function of the position $\mathbf{r}$ inside an insulator. Lorenz demonstrated that, provided that the dipole moment of each atomic cell varies appreciably only on the macroscopic scale, the link between the macroscopic polarization $\mathbf{P}(\mathbf{r})$ and the microscopic dipole moment $\boldsymbol{p}(\mathbf{r})$ of the primitive cell is expressed by:

$$\mathbf{P}(\mathbf{r}) = \boldsymbol{p}(\mathbf{r}) / \mathcal{V}$$

$\mathcal{V}$ is the equlibrium volume of the primitive cell.

Static response of a dielectric material to a steady electric field

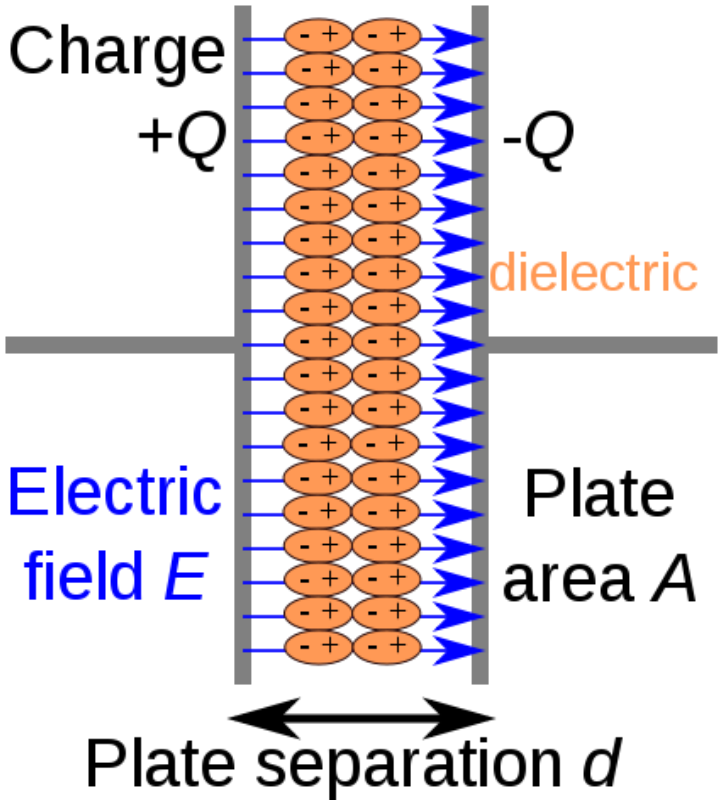

Static response of a dielectric material to a steady electric field represents only one part of the complete problem and, for practical purposes, actually a rather insignificant one. Time-dependent response to time-varying electric fields is more important from experimental and technological viewpoints.

Relation between permittivity, conductivity and dielectric loss

Most obvious physical reason for time-dependent dielectric response is the inevitable *inertia* of physical processes.

No material is able to follow arbitrarily fast varying driving forces. The consequence of the inertia is that the time-dependent polarisation *P*(t) is not the same function of time as the driving electric field *E*(t).

Time-dependent polarizability of a dielectric

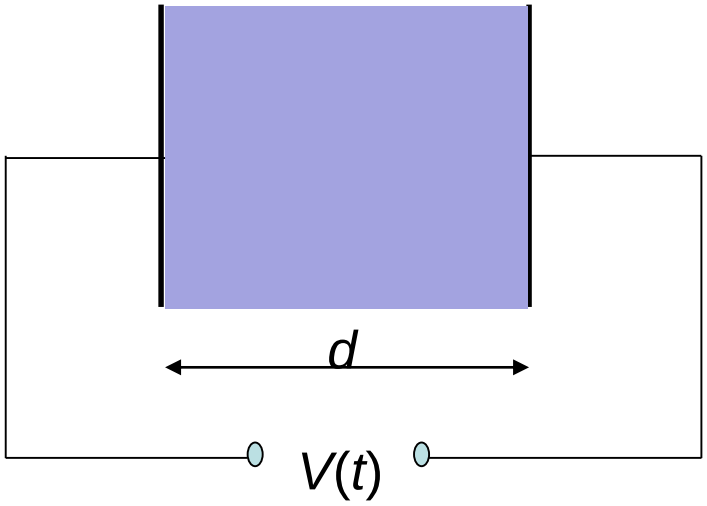

Spatially uniform electric field across the dielectric:

$$\boldsymbol{E(t)= V(t)/d}$$

The charges induced on the electrodes are the sum of an instantaneous free space contribution and the delayed material polarisation and the *dielectric displacement* is

$$\boldsymbol{D(t)=\varepsilon_0 E(t)+ P(t).}\ (1)$$

Relation between permittivity, conductivity and dielectric loss

For a linear dielectric system, for which the principle of superposition is valid, polarisation $P(t)$ is given by the convolution integral

$$P(t)=\varepsilon_0 \int_0^{\infty} f(\tau)E(t-\tau)d\tau \qquad (2)$$

- $f(t)$ is the dielectric response function describing mathematically the response of the dielectric medium to specific electric excitations
- $E(t)$ is the driving electric field

The physical meaning of the convolution is that the dielectric system has a memory of its past history and this may extend in practice to times as long as hours, days or even longer.

The polarisation after infinitely long charging time (under steady electric field E_0) is given by:

$$P(\infty)= P_0= \varepsilon_0 E_0 \int_0^{\infty} f(t)\, dt = \varepsilon_0 \chi(0) E_0 \qquad (3)$$

according to the definition of the steady-state dielectric susceptibility, $\chi(0)$.

Relation between permittivity, conductivity and dielectric loss

The frequency-domain response , that is the study of the response as a function of the excitation field frequency, relies on the Fourier transformation of a given function of time.
Fourier transform of a convolution integral is given by the product of the Fourier transforms of the two functions under the integral.
Applied to the time-dependent polarisation this theorem leads to:

$$FT[P(t)] = \mathcal{P}(\omega) = \varepsilon_0 \chi(\omega) \mathcal{E}(\omega) \qquad (4)$$

$\mathcal{P}(\omega)$- Fourier transform of time-dependent polarisation
$\mathcal{E}(\omega)$- Fourier transform of excitation field
$\chi(\omega)$- frequency-dependent susceptibility, defined as the transform of the response function $f(t)$

$$\chi(\omega) = \chi'(\omega) - i\chi''(\omega) = \int_0^\infty f(t) \exp(-i\,\omega\, t)dt \qquad (5)$$

Susceptibility is a complex function of frequency: it contains information not only about the amplitude but also about the phase angle of the the components of the polarisation.
Real part $\chi'(\omega)$ *gives the amplitude of the polarisation in phase with the excitation field*.
Imaginary part $\chi''(\omega)$ *gives the amplitude of the polarisation in quadrature with the driving field*.

Relation between permittivity, conductivity and dielectric loss

The physical significance of relation (4) $FT[P(t)] = \mathcal{P}(\omega) = \varepsilon_0 \chi(\omega)\, \mathcal{E}(\omega)$:

- replaces the convolution integral from the time-domain with the *simple* product of two functions from the frequency-domain, $\chi(\omega)\ \mathcal{E}(\omega)$,

- the frequency-dependent susceptibility $\chi(\omega)$ gives the response of the dielectric material to a harmonic excitation of frequency ω,

- simple measurement can yield $\chi(\omega)$ by exciting the system at the particular freq. ω,

- by sweeping the whole desired frequency range one may obtain the complete functional relationship.

The frequency-domain response of the dielectric system may be written in terms of dielectric permittivity, $\varepsilon(\omega)$:

$$D(\omega) = \varepsilon(\omega)E(\omega) = \varepsilon_0 [1 + \chi'(\omega) - i\chi''(\omega)]E(\omega) \qquad (6)$$

Real part of dielectric permittivity $\varepsilon'(\omega)$ consits of contributions from the free space and the dielectric itself; imaginary part of dielectric permittivity $\varepsilon''(\omega)$ is entirely made up by medium contributions.

Relation between permittivity, conductivity and dielectric loss

The current density that flows at a moment *t* through a dielectric is given by the direct current conductivity σ_0 and the dielectric displacement current:

$$I(t)=\sigma_0 E(t)+\partial D/\partial t \qquad (7)$$

Fourier- transform $I(t)$ and use $FT[\partial D/\partial t]= i\omega D(\omega)$,
where $D(\omega)$ is the Fourier transform of the time-dependent dielectric displacement $D(t)$ and are mathematically two different functions;
we obtain the frequency-domain relation:

$$\begin{aligned} \boldsymbol{I(\omega)} &= \sigma_0 E(\omega)+ i\omega D(\omega)= \sigma_0 E(\omega)+ i\omega[\varepsilon_0 E(\omega) + P(\omega)]= \\ &= \{\sigma_0+ i\omega\varepsilon_0[1+ \chi'(\omega)-i\chi''(\omega)]\} E(\omega) \\ &= \boldsymbol{\{[\sigma_0+ \omega\varepsilon_0\chi''(\omega)]\} + i\omega\varepsilon_0[1+ \chi'(\omega)\ ]\}E(\omega)} \qquad (8) \end{aligned}$$

- real part $\chi'(\omega)$ gives the component of the displacement current that flows *in quadrature with the excitation field* (thus not contributing to the power loss)
- imaginary part $\chi''(\omega)$ gives the component *in phase with the excitation field* and therefore contributes to the power loss→ $\chi''(\omega)$ is referred as the dielectric loss.

Relation between permittivity, conductivity and dielectric loss

Typically dielectric measurements are concerened with the movement of charge carriers, that is with electric current.

From Eqn. (8) it follows that the d.c. contribution refelected by σ_0 must appear in the measurement result, since the instrument cannot discriminate between the *true* dielectric response which does not contain σ_0 and the *effective* which does.
We can rewrite Eqn. (8)

$$I(\omega) = i\omega\varepsilon_{eff}(\omega)\, E(\omega) \qquad (9)$$

where $\varepsilon_{eff}(\omega)$ denotes the effective dielectric permittivity as measured by the instrument and is given by

$$\varepsilon_{eff}(\omega) = \varepsilon'(\omega) - i\,[\varepsilon''(\omega) + \sigma_0 / \omega]$$
$$= \varepsilon_0 \{1 + \chi'(\omega) - i\,[\chi''(\omega) + \sigma_0 / (\varepsilon_0 \omega)]\} \qquad (10)$$

From Eqn. (10) appears clearly that the d.c. conductivity σ_0 makes contribution to the apparent dielectic loss measured by a bridge system or other instrument, which diverges towards zero frequency.

A dielectric response in which $\varepsilon''(\omega) \propto 1/\omega$, while $\varepsilon'(\omega) \rightarrow$ const. as $\omega \rightarrow 0$ is a clear proof that the dominant process is direct current conduction in the relevant frequency range.

Kramers-Kronig relations

The real and imaginary part of the complex dielectric permittivity are not independent. It should be possible to find the ultimate relationships that bind the real and the imaginary part of the dielectric susceptibility, and are the *Kramers-Kronig formulae*. Eqn. (6) was derived for a *linear* dielectric system and for which the causality principle was valid, which will allow the extension of the lower limit of integration to -∞.

Whence the resulting Kramers-Kronig relationships have restricted applicability to linear systems and are ultimately a consequence of causality principle:

Real part of susceptibility

$$\chi_1(\omega) = \frac{1}{\pi}\mathcal{P}\int_{-\infty}^{\infty} \frac{\chi_2(\omega')}{\omega' - \omega}\, d\omega' \qquad (11a)$$

Imaginary part of susceptibility

$$\chi_2(\omega) = -\frac{1}{\pi}\mathcal{P}\int_{-\infty}^{\infty} \frac{\chi_1(\omega')}{\omega' - \omega}\, d\omega', \qquad (11b)$$

or $$\chi_1(\omega) = \frac{2}{\pi}\mathcal{P}\int_{0}^{\infty} \frac{\omega'\chi_2(\omega')}{\omega'^2 - \omega^2}\, d\omega'. \qquad (12a)$$

$$\chi_2(\omega) = -\frac{2}{\pi}\mathcal{P}\int_{0}^{\infty} \frac{\omega\chi_1(\omega')}{\omega'^2 - \omega^2}\, d\omega' = -\frac{2\omega}{\pi}\mathcal{P}\int_{0}^{\infty} \frac{\chi_1(\omega')}{\omega'^2 - \omega^2}\, d\omega'. \qquad (12b)$$

$\mathcal{P}$ integrals denote the Cuachy principal value of the integrals

K-K relations give either $\chi'(\omega)$ or $\chi''(\omega)$ at a particular value of the frequency in terms of the integral transform of the other throughout the entire frequency range (-∞, ∞).

Relation between permittivity, conductivity and dielectric loss
Kramers-Kronig relations

A very direct consequence of the K-K relations is their assessment for zero-frequency:

$$\chi'(0) = \frac{2}{\pi}\int_0^\infty \frac{\chi''(x)}{x}\,dx = \frac{2}{\pi}\int_0^\infty \chi''(x)\;d(\ln x) \qquad (13)$$

Eqn. (13) relates the polarisation increment for a given polarisation mechanism or combination of mechanisms to the area of the loss curve plotted against the natural logarithm of frequency.

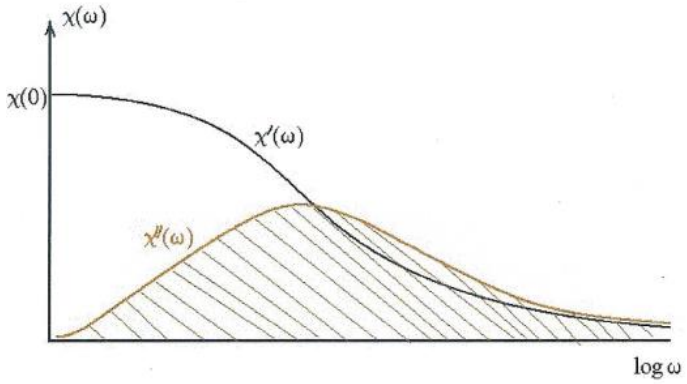

A polarisation mechanism that leads to a strong polarisation must give rise to correspondingly high dielectric losses somewhere in the frequency spectrum.
It is impossible to have a dispersion-free dielectric material, i.e. one that has frequency-independent real and imaginary parts of the susceptibility.
Variation of the dielectric permittivity with frequency, known as dispersion, is a fundamental property of all dielectric materials.

Polarization mechanisms

For most dielectrics their dielectric loss is significant only in certain limited ranges of frequency. $\chi'(\omega)$ is almost frequency-independent outside the regions with important loss.

A high frequency permittivity is often defined, as ε_∞. It is given by the free space contribution ε_0 and of the contribution of all the other polarizing mechanisms at higher frequencies, and eqn. (10) can be rewritten for any such polarization process α as:

$$\varepsilon(\omega) = \varepsilon_{\infty\alpha} + \varepsilon_0 [\chi'(\omega) - i\chi''(\omega)] \qquad (14)$$

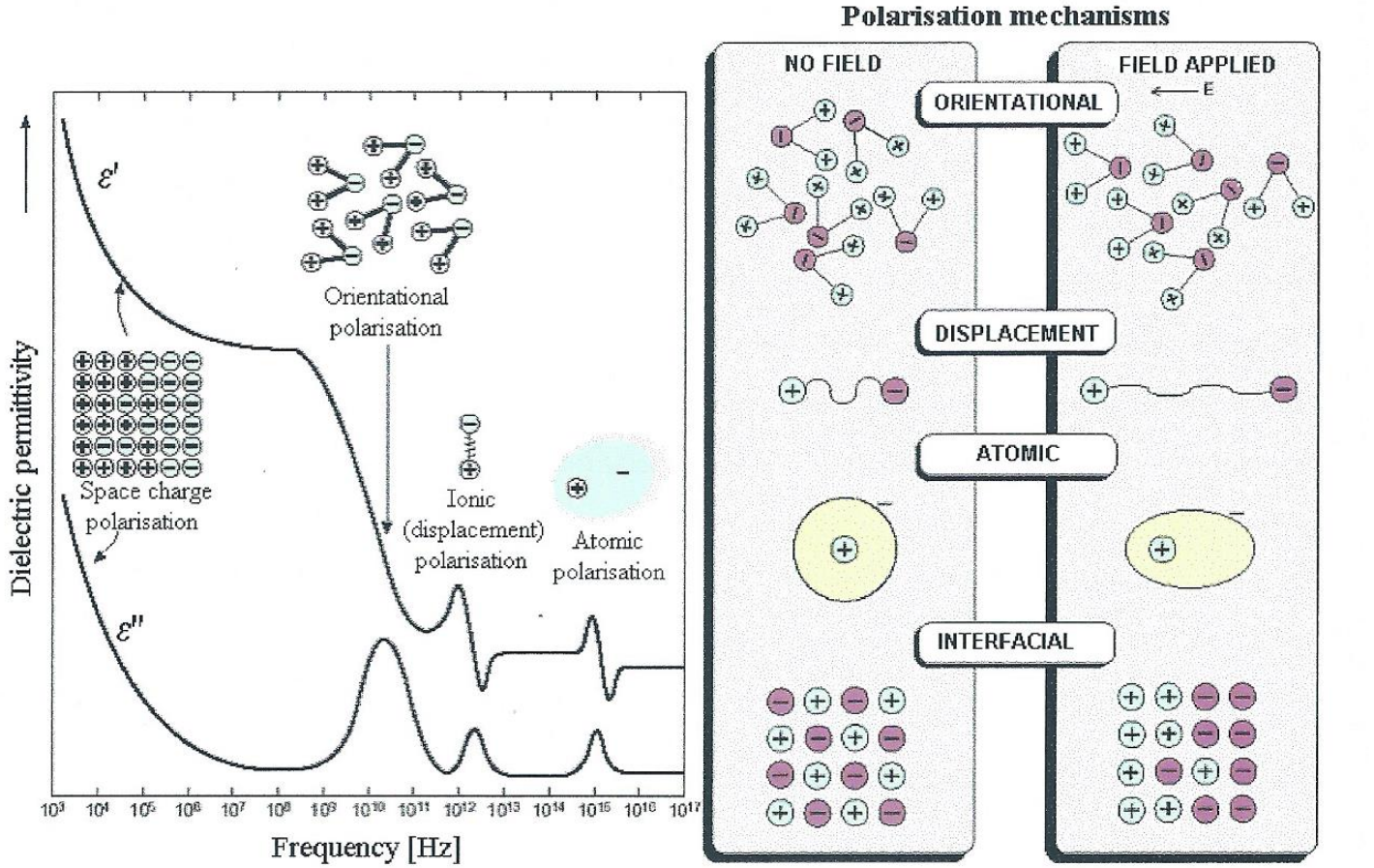

Theories of the local field and of the polarizability

It is necessary to relate the polarization density **P(r)** to macroscopic electric field **E(r)**.

Due to ion microscopic dimensions, ionic displacement and distortion are determined by the force due to the *microscopic* field at the position of the ion, diminished by the contribution to the microscopic field from the ion itself. This is the local (or effective) field, $\mathbf{E}^{loc}(\mathbf{r})$.

For a basic evaluation of $\boldsymbol{E^{loc}(r)}$ *see for instance Chapter 27 in Ashcroft & Mermin.*

For the case when every equilibrium site in the equilibrium crystal is *a center of cubic symmetry* we get the **Lorentz relation**:

$$\mathbf{E}^{loc}(\mathbf{r}) = \mathbf{E}(\mathbf{r}) + (\boldsymbol{\varepsilon}_0)^{-1}\,\mathbf{P}(\mathbf{r})/3$$

Or, in terms of dielectric constant of the *cubic* medium, using the constitutive relation

$$\mathbf{D}(\mathbf{r}) = \varepsilon\,\mathbf{E}(\mathbf{r}) = \boldsymbol{\varepsilon}_0\,\mathbf{E}(\mathbf{r}) + \mathbf{P}(\mathbf{r}) \rightarrow \mathbf{P}(\mathbf{r}) = (\varepsilon - \boldsymbol{\varepsilon}_0)\mathbf{E}(\mathbf{r})$$

$$\rightarrow \boxed{\mathbf{E}^{loc}(\mathbf{r}) = (\varepsilon + 2\,\boldsymbol{\varepsilon}_0)\mathbf{E}(\mathbf{r})/(3\boldsymbol{\varepsilon}_0)}$$

Polarizability α of a medium

Polarizability $\alpha(\mathbf{d})$ of the type of ion at position **d** in the basis is the ratio of its induced dipole moment to the field actually acting on it.
The polarizability of the medium is the sum of the polarizabilities of the ions in a primitive cell.

It can be shown that

$$\mathbf{P}(\mathbf{r}) = \alpha \mathbf{E}^{loc}(\mathbf{r}) / \mathcal{V}$$

And it follows that

N density of dipoles

$$\frac{\varepsilon - \boldsymbol{\varepsilon}_0}{\varepsilon + 2\boldsymbol{\varepsilon}_0} = \frac{N\alpha}{3}$$

Clausius-Mossotti relation

A microscopic theory is required to calculate α, which gives the response of the ions to the actual field $\mathbf{E}^{loc}(\mathbf{r})$ acting on them.

The resulting ε can be used together with the Maxwell equations to predict the OPTICAL PROPERTIES of an insulator.

Induced dipole moment at position **d** in the ionic basis (**R**- Bravais lattice site)**:**

$$\underbrace{\mathbf{p}(\mathbf{R}+\mathbf{d})}_{\text{atomic polarizability}} + \underbrace{e\mathbf{u}(\mathbf{R}+\mathbf{d})}_{\text{displacement polarizability}} = \alpha(\mathbf{d})\, \mathbf{E}^{\text{loc}}(\mathbf{r})\Big|_{\mathbf{r}\approx\mathbf{R}}$$

Atomic polarizability- due to distorsions of the ionic charge distribution
Displacement polarizability- due to ionic displacements; important in ionic crystals

Atomic polarizability

We allow the local field acting on the ion to be frequency-dependent: $\mathbf{E}^{\text{loc}} = \text{Re}(\mathbf{E_0} e^{-i\omega t})$

A crude classical model to estimate the frequency dependence of the polarizability of an ion (see derivation of Ashcroft&Mermin) treats the ion as an electronic shell of charge $Z_i e$ and mass $Z_i m$, tied to a heavy immobile, undeformable ion core, by a harmonic spring of spring constant $K = Z_i m \omega_0^2$

$$\alpha^{\text{at}}(\omega) = \frac{Z_i e^2}{m(\omega_0^2 - \omega^2)}$$

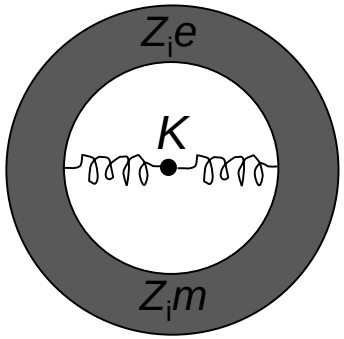

If ω is small compared to ω_0, the atomic polarizability will be independent of frequency and its static value is:

$$\alpha^{\text{at}} = \frac{Z_i e^2}{m\omega_0^2}$$

Atomic polarizability

It is expectable that ω_0 is of the order of an atomic excitation energy devided by $\hbar$.
We can estimate the frequency below which α^{at} will be frequency-independent:

$$\hbar\omega_0 = \sqrt{\frac{\hbar^2 Z_i e^2}{m\alpha^{at}}}$$

$$\hbar\omega_0 = \sqrt{Z_i \frac{10^{-24}\ \mathrm{cm}^3}{\alpha^{at}}} \times 10.5\ \mathrm{eV}$$

Measured atomic polarizabilities are of the order 10^{-24} cm^3, so the frequency dependence of atomic polarizabilty will not come into play until frequencies corresponding to UV radiation.

Displacement polarizability

In ionic crystals we must consider the dipole moment due to the displacement of ions by the electric field.
Model:
- rigid-ion approximation (ignore the deformation of the electronic shells of the ions under the applied field)
- crystal with two ions per primitive cell, of charges *e* and *–e*

The dipole moment of the primitive cell is then $\mathbf{p} = e\mathbf{w}$, $\mathbf{w} = \mathbf{u}^+ - \mathbf{u}^-$, where $\mathbf{u}^+$, $\mathbf{u}^-$ are the displacement of the positive and negative ion from its equilibrium position.

Displacement polarizability

(from Ashcroft&Mermin, so GAUSS system of units!!!)

The relative displacement induced by a frequency-dependent local field $\mathbf{E}^{loc} = \mathrm{Re}(\mathbf{E_0} e^{-i\omega t})$:

$$\mathbf{w} = \mathrm{Re}\,(\mathbf{w}_0 e^{-i\omega t}),$$

$$\mathbf{w}_0 = \frac{eE_0/M}{\varpi^2 - \omega^2}$$

where M is the ionic reduced mass $M^{-1} = (M_+)^{-1} + (M_-)^{-1}$ and $\varpi^2 = k/M$.

Accordingly

$$\alpha^{dis} = \frac{p_0}{E_0} = \frac{ew_0}{E_0} = \frac{e^2}{M(\varpi^2 - \omega^2)}$$

The resonant frequency ϖ is characteristic of lattice vibrational frequencies and therefore $\hbar\varpi \approx 10^{-1}$ to 10^{-2} eV. This can be 100 to 1000 times smaller than the atomic frequency, ω_0, and thus the displacement polarizability has a significant frequency dependence in the infrared and optical range.

NOTE: ionic mass M is about 10^4 times the electronic mass m, so the static ($\omega = 0$) atomic and displacement polarizabilities may well be of the same size, so a *naive* completion of α^{dis} would be:

$$\alpha^{dis} = (\alpha^+ + \alpha^-) + \frac{e^2}{M(\varpi^2 - \omega^2)}$$

α^+ and α^- are the atomic polarizabilties of the positive and negative ions

Dielectric permittivity of ionic crystals

Dielectric permittivity of an ionic crystal, given by the Clausius-Mossotti relation:

$$\frac{\varepsilon(\omega)-1}{\varepsilon(\omega)+2} = \frac{4\pi}{3v}\left(\alpha^{+} + \alpha^{-} + \frac{e^2}{M(\varpi^2-\omega^2)}\right)$$

In particular:

Static dielectric constant is ($\omega << \varpi$):

$$\frac{\varepsilon_0-1}{\varepsilon_0+2} = \frac{4\pi}{3v}\left(\alpha^{+} + \alpha^{-} + \frac{e^2}{M\varpi^2}\right)$$

High-frequency dielectric constant (i.e. high compared with the lattice vibrational frequencies, ($\varpi << \omega << \omega_0$):

$$\frac{\varepsilon_\infty-1}{\varepsilon_\infty+2} = \frac{4\pi}{3v}\left(\alpha^{+} + \alpha^{-}\right)$$

ε_∞ is the dielectric constant at optical frequencies and related to the index of refraction, n, $n^2 = \varepsilon_\infty$

We can rewrite as:

$$\frac{\varepsilon(\omega)-1}{\varepsilon(\omega)+2} = \frac{\varepsilon_\infty-1}{\varepsilon_\infty+2} + \frac{1}{1-(\omega^2/\varpi^2)}\left(\frac{\varepsilon_0-1}{\varepsilon_0+2} - \frac{\varepsilon_\infty-1}{\varepsilon_\infty+2}\right)$$

We end up with:

$$\boxed{\varepsilon(\omega) = \varepsilon_\infty + \frac{\varepsilon_\infty-\varepsilon_0}{\left(\frac{\omega^2}{\omega_T^2}\right)-1}}$$

where $\omega_T^2 = \varpi^2\left(\frac{\varepsilon_\infty+2}{\varepsilon_0+2}\right) = \varpi^2\left(1-\frac{\varepsilon_0-\varepsilon_\infty}{\varepsilon_0+2}\right)$

Long-wavelength optical modes of ionic crystals

(from Ashcroft&Mermin, so GAUSS system of units!!!)

In **long-wavelength optical modes** ($k \approx 0$) of IONIC CRYSTALS: the oppositely charged ions in each primitive cell undergo oppositely directed displacements, giving rise to a nonvanishing polarization density **P**, and $\mathbf{D} = \varepsilon \mathbf{E} = \mathbf{E} + 4\pi\mathbf{P}$
(no free charges) $\nabla \cdot \mathbf{D} = 0$,
$\nabla \times \mathbf{E} = \nabla \times (-\nabla \Phi) = 0$ (may be inaccurate at optical frequencies)

In a *cubic* ionic crystal **D** II **E** (ε is a scalar) and thus both are parallel to **P**
Longitudinal optical mode: **P** II $\boldsymbol{k} \rightarrow \mathbf{E} = -4\pi\mathbf{P}$ and $\varepsilon = 0$
Transverse optical mode: **P** $\perp k \rightarrow \mathbf{E} = 0$ and $\varepsilon = \infty$

According to the dispersion relation, $\varepsilon = \infty$ when $\omega^2 = \omega_T^2$,
so ω_T is identified as the frequency of the long-wavelength transverse optical mode.

And for the longitudinal optical mode $\varepsilon = 0$, so ω_L

$$\omega_L^2 = \frac{\varepsilon_0}{\varepsilon_\infty}\omega_T^2$$

Lyddane-Sachs-Teller relation

Since the crystal is more polarizable at lower frequencies ($\varepsilon_0 > \varepsilon_\infty$) $\rightarrow$ $\omega_L > \omega_T$

Frequency-dependent dielctric constant for a diatomic ionic crystal

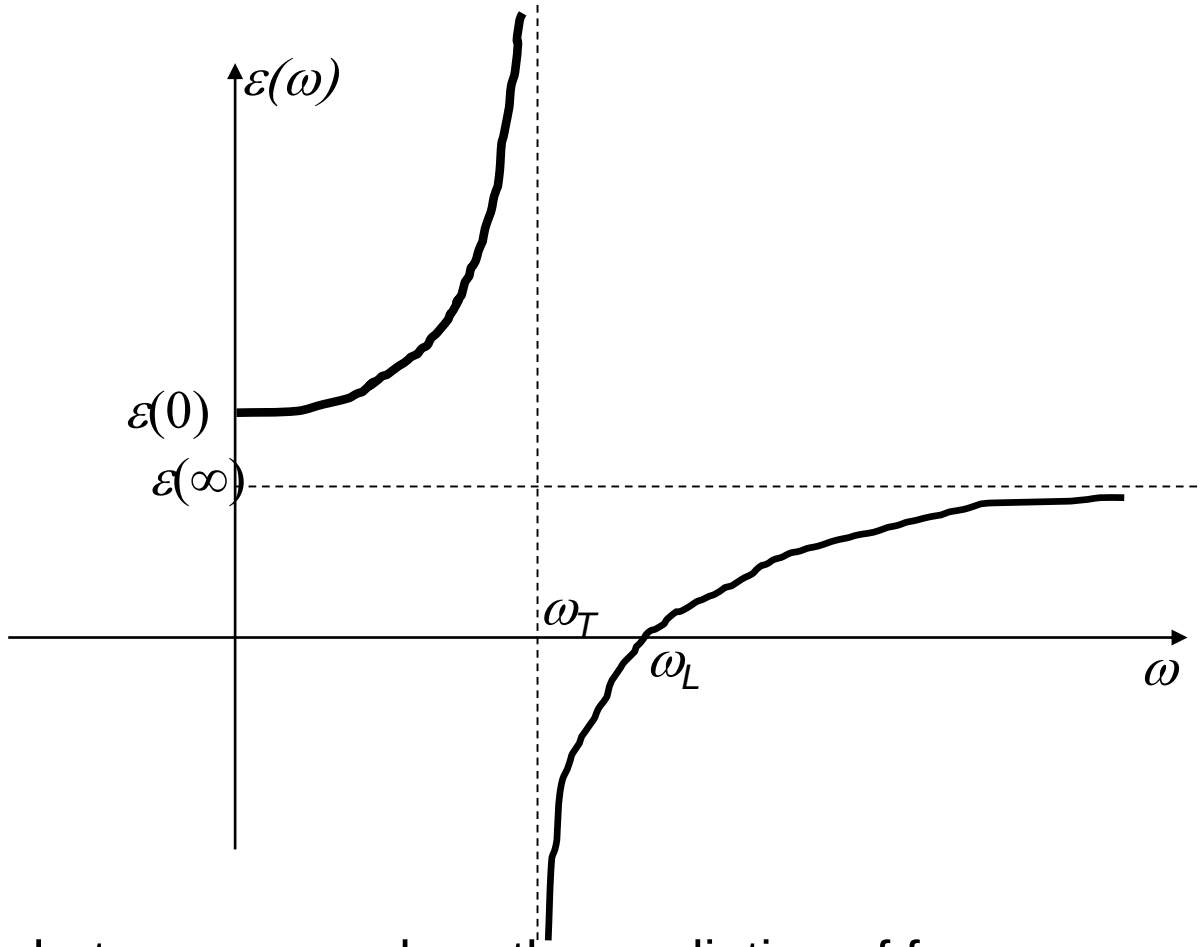

ε is negative between ω_T and ω_L, thus radiation of frequency ω between transverse and optical frequencies cannot propagate in the crystal (Multiple reflections of radiation results in a *reststrahl* –way of measuring very precise ω_T and of producing very monochromatic infrared radiation)

FERROELECTRICS

Why are ferroelectrics and especially their thin films interesting?

The various unique properties of ferroelectric thin films:

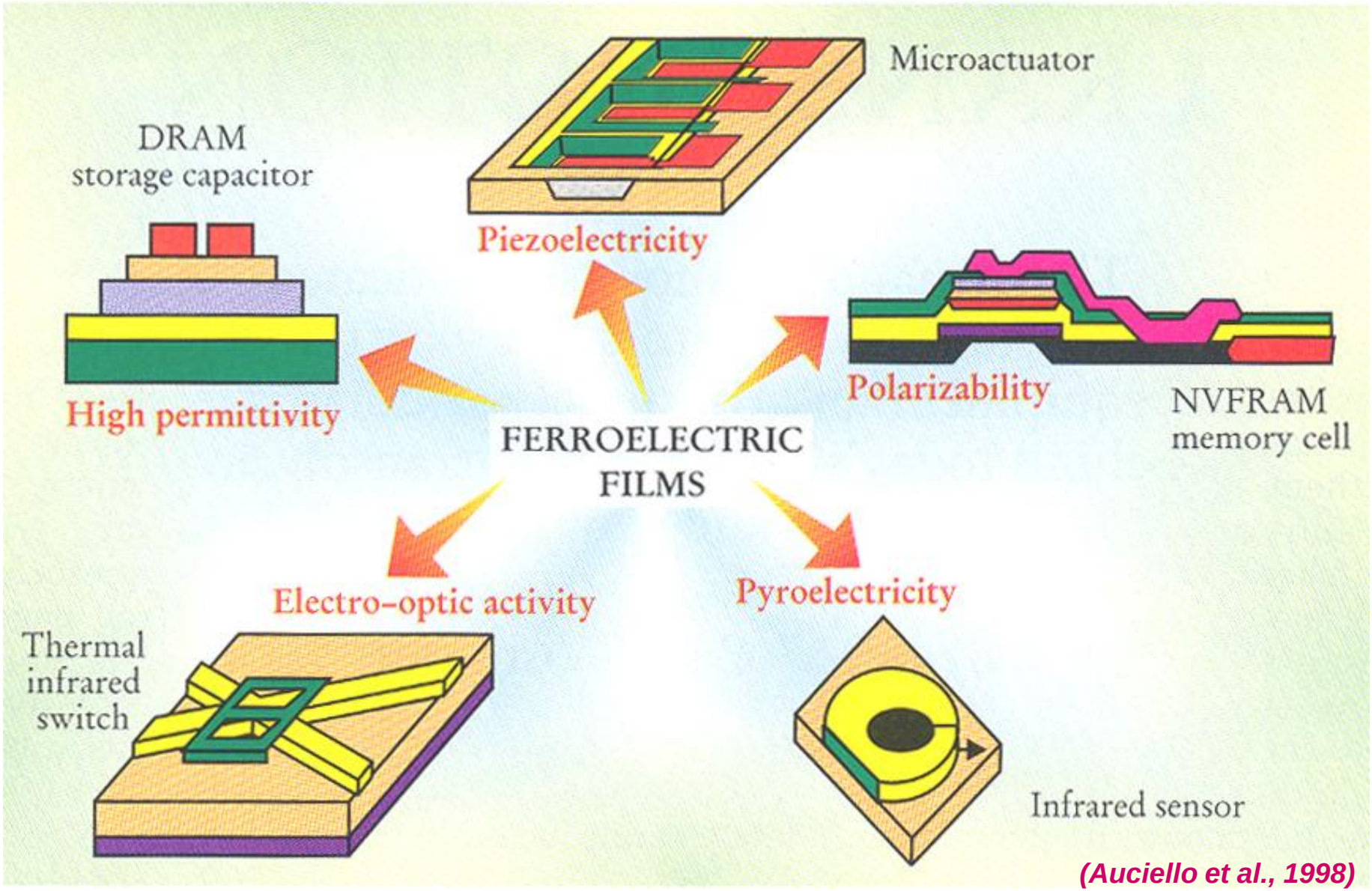

(Auciello et al., 1998)

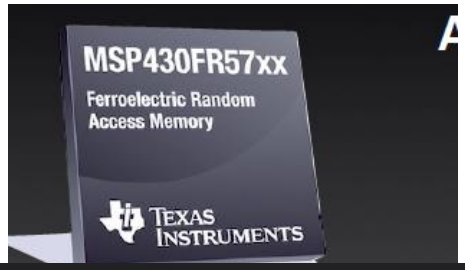

Thanks to *J. M. Triscone*, University of Geneve

Ferroelectric RAM's for smart cards and portable electronic devices

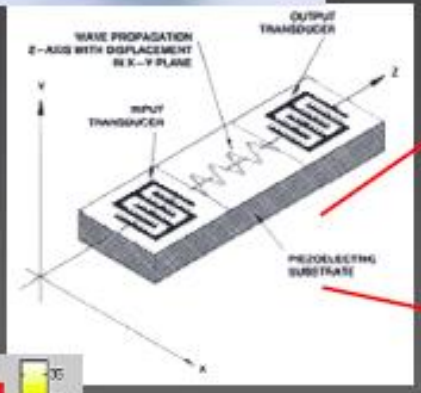

Thermal IR pyroelectric detectors

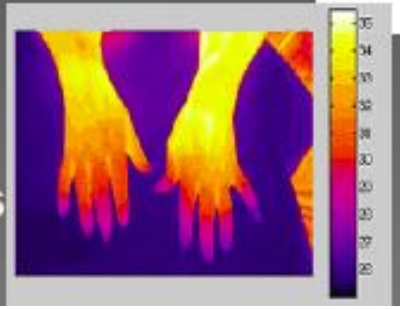

SAW devices for mobile technology and gas sensing

DEFINITIONS

Ferroelectric: a *crystal* is said to be ferroelectric when it has two or more discrete stable or metastable states of different nonzero electric polarization, in zero applied electric field, referred to as "spontaneous polarization", and it must be possible to switch between these states with a suitably large applied electric field.

The mechanism of *switching the polarization* is understood to take place on scales larger than the unit-cell scale, and generally to require the nucleation, growth and shrinking of *domains* through the motion of *domain walls*.

The observation of an *electric hysteresis P-E loop* is considered necessary to estabilish ferroelectricity.

Any of the two of the orientation states are identical (or entatiomorphous) in crystal structure and differ only in electric polarization vector at null electric field.

Ferroelectric hysteresis

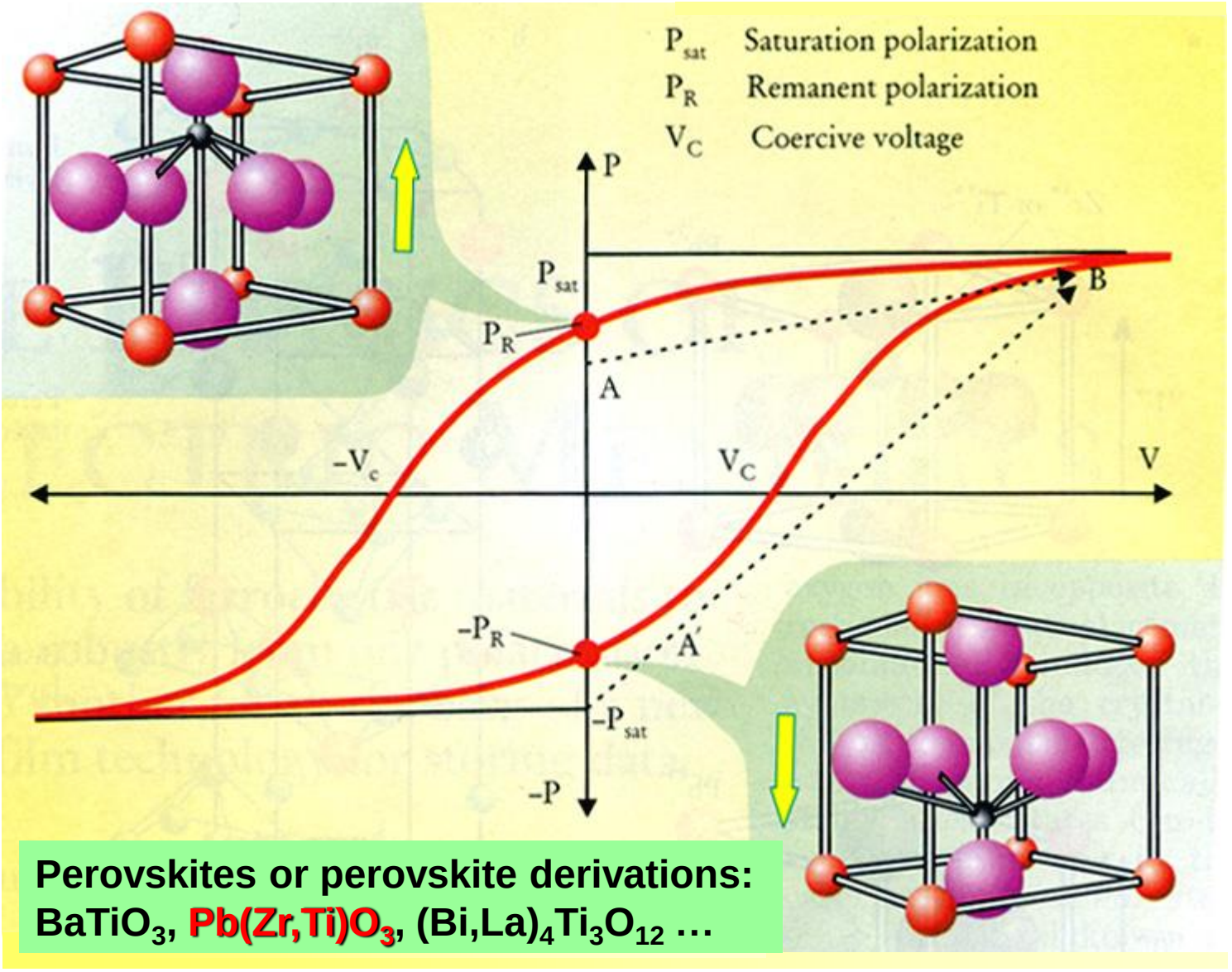

Perovskites or perovskite derivations:
$BaTiO_3$, $Pb(Zr,Ti)O_3$, $(Bi,La)_4Ti_3O_{12}$ …

Record ferroelectric polarization (100 μC/cm^2) is held by $PbZr_{0.2}Ti_{0.8}O_3$ and $BiFeO_3$ **epitaxial thin films** (bulk single crystals do not exist for the PZT and are difficult to get for BFO)

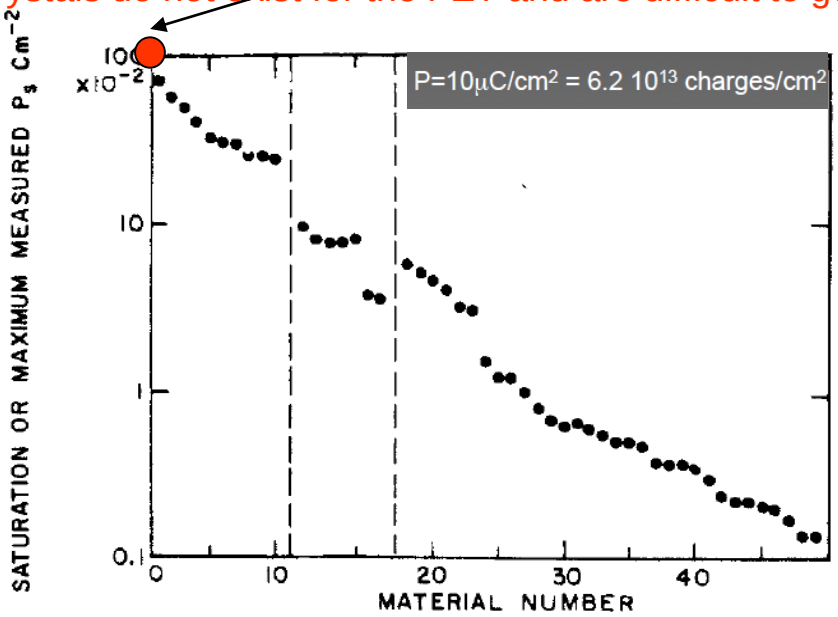

FIGURE 12 Spontaneous polarization of some ferroelectric materials. Broken lines separate one-, two- and three-dimensional classes. Materials are arranged as follows:

1. $LiNbO_3$
2. $PbTiO_3$
3. $LiTaO_3$
4. $Ba_4Na_2Nb_{10}O_{30}$
5. $Ba_{1.3}Sr_{3.7}Nb_{10}O_{30}$
6. $KNbO_3$
7. $Pb(Fe_{\frac{1}{2}}Ta_{\frac{1}{2}})O_3$
8. $BaTiO_3$
9. SbSI
10. $Pb(Mg_{\frac{1}{3}}Nb_{\frac{2}{3}})O_3$
11. $BaZnF_4$
12. $BaCoF_4$
13. $BaMgF_4$
14. $BaNiF_4$
15. $NaNO_2$
16. HCl
17. $SC(NH)_2$
18. RbH_2PO_4
19. KH_2AsO_4
20. KH_2PO_4
21. $(NH_2CH_2COOH)_3 \cdot H_2BeF_4$
22. $(NH_2CH_2COOH)_3 \cdot H_2SO_4$
23. $P(CH_3)_4HgBr$
24. $(NH_2CH_2COOH)_2 \cdot HNO_3$
25. $N(CH_3)_4HgI_3$
26. $N(CH_3)_4HgCl_3$
27. $N(CH_3)_4HgBr_3$
28. NH_4HSO_4
29. $RbHSO_4$
30. $NH_2CH_2COOH \cdot AgNO_3$
31. $CaB_3O_4(OH)_3 \cdot H_2O$
32. $C(NH_2)_3Ga(SeO_4)_2 \cdot 6H_2O$
33. $C(NH_2)_3Al(SeO_4)_2 \cdot 6H_2O$
34. $C(NH_2)_3Ga(SO_4)_2 \cdot 6H_2O$
35. $(NH_4)_2SO_4$
36. $C(NH_2)_3Cr(SeO_4)_2 \cdot 6H_2O$
37. $C(NH_2)_3V(SO_4)_2 \cdot 6H_2O$
38. $C(NH_2)_3Cr(SO_4)_2 \cdot 6H_2O$
39. $NaKC_4H_4O_6 \cdot 4H_2O$
40. $C(NH_2)_3Al(SO_4)_2 \cdot 6H_2O$
41. $Ca_2Sr(CH_3CH_2COO)_6$
42. $Sm_2(MoO_4)_3$
43. $LiNH_4C_4H_4O_6 \cdot H_2O$
44. $(NH_4)_2BeF_4$
45. $NaNH_4C_4H_4O_6 \cdot 4H_2O$
46. $Tb_2(MoO_4)_3$
47. $Gd_2(MoO_4)_3$
48. $Eu_2(MoO_4)_3$
49. $LiTlC_4H_4O_6 \cdot H_2O$

S. C. Abrahams and E. T. Keve, Ferroelectrics 2,129 (1971)

History (1) :

First experienced phenomenon related to ferroelectricity was PYROELECTRICITY- *possesion by some materials of temperature-dependent spontaneous electric dipole moment*, known since ancient times because of the ability of such materials to attract objects when they were heated.

Small temperature change ΔT, uniform over the crystal, the change of the polarization vector ΔP_i is given by

$$\Delta P_i = p_i \Delta T$$

Where p_i are the 3 pyroelectric coefficients. The pyroelectric effect in a crystal is thus specified by the vector $\boldsymbol{p}$.

Studies of pyroelectricity (18th-19th century) on materials such as tourmaline eventually led to the discovery of PIEZOELECTRICITY

1880, J. Curie and P. Curie - piezoelectric effect, *production of electrical polarity (charge) by application of stress*: the Curies realized that the difference between the charge developed upon uniform and non-uniform heating was due to the thermal stress created in the pyroelectric)

$$P_i = d_{ijk}\ \sigma_{jk}$$

The d_{ijk} are the piezoelectric moduli (27 coefficients of a third-rank tensor)

None of the early known pyroelectric materials were FERROELECTRIC, *in the sense of possesing an electrically REORIENTABLE ELECTRIC MOMENT*.

The 32 crystallographic point groups arranged by crystal systems

Crystal system	Symbol: International	Symbol: Schoenflies	Pyroelectric	Piezoelectric	Centrosymmetric
Triclinic	1	C_1	√	√	
	$\bar{1}$	C_i			√
Tetragonal	4	C_4	√	√	
	$\bar{4}$	S_4		√	
	4/m	C_{4h}			√
	422	D_4		√	
	4mm	C_{4v}		√	
	$\bar{4}$2m	D_{2d}		√	
	4/mmm	D_{4h}			√
Hexagonal	6	C_6		√	
	$\bar{6}$	C_{3h}		√	
	6/m	C_{6h}			
	622	D_6		√	
	6mm	C_{6v}	√	√	
	$\bar{6}$m2	D_{3h}		√	
	6/mmm	D_{6h}			√
Monoclinic	2	C_2	√	√	
	m	C_s	√	√	
	2/m	C_{2h}			√
Orthorhombic	222	D_2		√	
	mm2	C_{2v}	√	√	
	mmm	D_{2h}			√
Trigonal	3	C_3	√	√	
	$\bar{3}$	S_6			√
	32	D_3		√	
	3m	C_{3v}	√	√	
	$\bar{3}$m	D_{3d}			√
Cubic	23	T		√	
	m3	T_h			√
	432	O			
	$\bar{4}$3m	T_d		√	
	m3m	O_h			√

A tick (√) indicates that the point group is pyroelectric, piezoelectric, or centrosymmetric, as the case may be.

From *Lines&Glass, Principles and Applications of Ferroelectrics*

1920, Valasek: Rochelle salt

($NaKC_4H_4O_6 \cdot 4H_2O$)- its polarization could be reversed by application of an electric field.

First display of ferroelectric behavior!

The crystal structure of Rochelle salt (sodium potassium tartrate tetrahydrate $NaKC_4H_4O_6 \cdot 4H_2O$)

By C. A. Beevers and W. Hughes

(*Communicated by W. L. Bragg, F.R.S.—Received* 1 *August* 1940)

The complete crystal structure of Rochelle salt (sodium potassium tartrate tetrahydrate) has been determined by Fourier and Patterson methods. Some of the difficulties in the application of these methods are discussed.

The tartrate molecule is found to lie approximately in three planes, the planes of each half of the molecule being inclined at 60° to the plane of the carbon atoms. The tartrate molecules are bonded to sodium and potassium atoms both directly and through the medium of water molecules. If the water molecules are to preserve their customary tetrahedral 'bonding' it is necessary to suppose that one of the carboxyl groups of the molecule is also a dipole. A reversal of the continuous chain of carboxyl-water-water dipoles is a possible explanation of the peculiar dielectric properties of the salt.

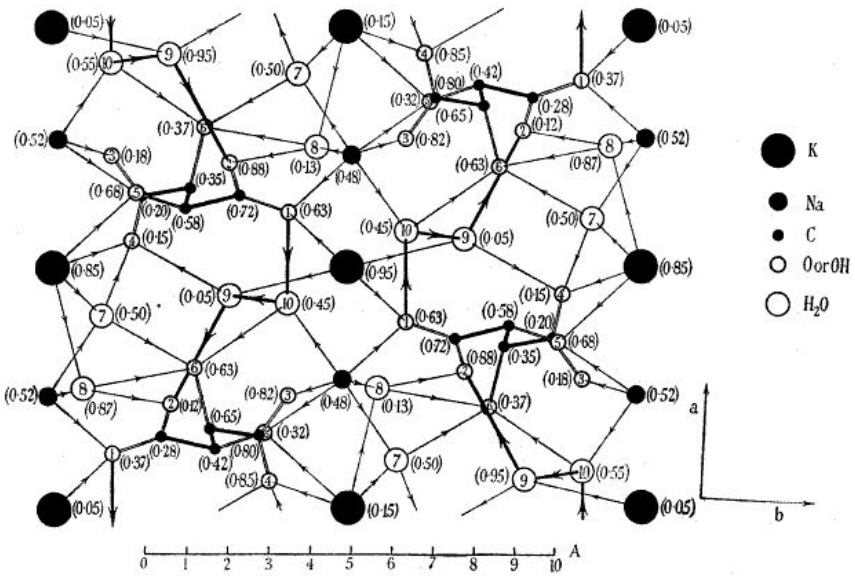

Figure 1. Projection on (001) plane, of the structure of Rochelle salt. The arrow heads on the bonds are drawn in a direction from positive atoms to negative atoms. The bonds involved in the 1–2–9–10 chains are drawn thick, so that the chains can be picked out.

Table 1

2 K on (*a*)		(0·00	0·00	0·05)
2 K on (*b*)		(0·00	0·50	0·15)
4 Na on		(0·23	0·99	0·52)
4 O on	(1)	(0·12	0·10	0·37)
4 O on	(2)	(0·22	0·20	0·12)
4 O on	(3)	(0·23	0·40	0·82)
4 O on	(4)	(0·06	0·37	0·85)
4 OH on	(5)	(0·16	0·36	0·32)
4 OH on	(6)	(0·29	0·24	0·63)
4 H_2O on	(7)	(0·40	0·08	0·50)
4 H_2O on	(8)	(0·25	0·05	0·87)
4 H_2O on	(9)	(0·44	0·30	0·05)
4 H_2O on	(10)	(0·42	0·40	0·45)
4 C on		(0·15	0·18	0·28)
4 C on		(0·12	0·28	0·42)
4 C on		(0·17	0·27	0·65)
4 C on		(0·15	0·35	0·80)

History (2) : discovery of more ferroelectrics

SLOW acceptance of ferroelectricity as a subject worthy of more general study was the fact that ANY SMALL DEVIATIONS FROM THE CORRECT CHEMICAL COMPOSITION of Rochelle salt seemed to destroy ferroelectricity, leading to experimental problems of reproducibility and a GROWING CONVICTION THAT THIS WAS ONE OF NATURE'S GREAT ACCIDENTS!

1935-1938, Busch and Scherrer: first series of ferroelectric crystals were produced, the greatest significance of this event was the discovery of a whole set of series of isomorphous crystals and not just an isolated example - phosphates and arsenates, the prototype being

- KH_2PO_4 (KDP): with a single transition at T_C~ 122 K.
- $NH_4H_2PO_4$(ADP): did not seem to have a net spontaneous polarization below T_C — it is ANTIFERROELECTRIC!

Like Rochelle salt, KDP and ADP remain piezoelectric even after their ferroelectric/paraelectric transition → most of the technical applications focused on their peizoelectric rather than ferroelectric properties: ADP has 30% electromechanical coupling efficiency at RT, it was the principal material for underwater sound transducer and submarine detectors in World War II, replacing the very temperature-dependent Rochelle salt.

KDP and ADP: their crystal structure is also simpler than Rochelle salt and thus easier to be treated theoretically. For the next decade it was thought quite likely that the existance of hydrogen bonds was necessary, if not sufficient, condition for the polar instability to occur.

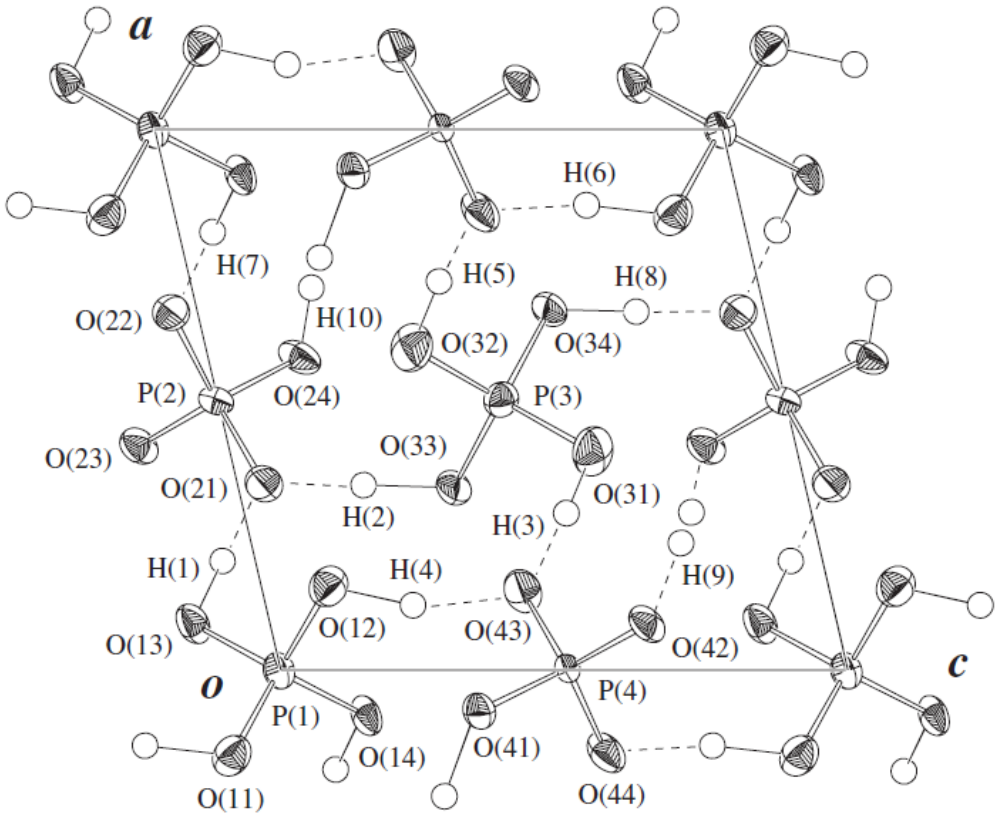

Fig. 1. Projection on the *ac*-plane of monoclinic KDP structure at 297 K with 60% probability displacement ellipsoids.

Journal of the Physical Society of Japan
Vol. 75, No. 7, July, 2006, 074602

History (3): discovery of perovskite oxide ferroelectrics, barium titanate $BaTiO_3$

1945-1946, Wul and Goldman: barium titanate $BaTiO_3$ (BTO) with perovskite structure was found to have a dielectric constant of 1000 to 3000 at RT and even higher as temperature raised.
Soon after, ferroelectricity was reported in BTO, hence hydrogen hypothesis of ferroelectricity had to be abandoned.

$BaTiO_3$ is the
- 1st ferreoelectric without hydrogen bond
- 1st ferreoelectric with more than one ferroelectric phase
- 1st ferreoelectric with a non-piezoelectric prototype / paraelectric phase

Crystal structure of the prototype phase was cubic centrosymmetric with very high symmetry and the unit cell has only 5 atoms!!!
- encouraging for the theorists!
- became the forerunner of the largest single class of all ferroelectrics, the oxygen octahedral ferroelectrics made up of basic BO_6 building blocks

History (4): theoretical progress at the MACROscopic level

Phenomenologic (thermodynamic) theory of ferroelectrics

PHENOMENOLOGICAL or macroscopic theories of dielectrics (and ferroelectrics in particular) treat the material in question as a continuum disregarding any underlying atomic structure.

Theory had progressed more rapidly by focusing mainly on thermodynamic concepts, due to the ability to relate macroscopic measureables and to include with ease changes of external constraints, such as *stress*.

There is a distinct difference between ferromagnetic (FM) and ferroelectric (FE) theories in that one can nearly always neglect mechanical coupling in the FM (magnetostrictive effects are usually in parts per million), whereas strains associated with the onset of ferroelectricity are often of essential importance, at 1 % or larger.

Phenomenologic (thermodynamic) theory of ferroelectrics

Energy function capable of describing both polar and non-polar phases: approach perfected in 1949-1954 by Ginzburg and Devonshire, with specific reference to $BaTiO_3$ (for which the accumulation of an immense amount of experimental data, coupled with the occurrance of three different FE phases with different polar axes, enabled a thorough test of the method).

Fields are postulated in sufficient number to describe the thermal, elastic, and dielectric properties of the macroscopic system.
The laws of thermodynamics and classical mechanics are used to obtain the relationships between them.

The dielectric system is possible to be described by three independent variables chosen from the pairs:

(temperature *T*, entropy *S*)
(stress *X*, strain *x*)
(Maxwell field *E*, dielectric displacment *D*)

Coupling between the order parameter, i.e. polarization *P*, and strain *x* is usually large enough in FE to be considered.

Second-order FE phase transition

Thermodynamic potentials, e.g. elastic Gibbs energy G_1:

$G_1 = U - TS - X_i x_i$

In the prototype (non-polar) state, (1) $D_i=0$, $x_i=0$; (2)$D_i=D$ is oriented along one of the crystallographic axes only;(3) all stresses $X_i=0$; (4) non-polar phase is centosymmetric) we can write:

$G_1 = (\alpha/2)D^2+(\gamma/4)D^4+(\delta/6)D^6$

G_1 is measured from the non-polar (prototype) phase and the coefficients γ,δ are temperature-independent.

Phase transition's order depends on the sign of γ →**for γ, δ> 0: second-order phase transition**

The Maxwell field *E* (parallel to *D)* is $E=(\partial G_1/\partial D)_T$:

$E = \alpha D+\gamma D^3+\delta D^5$

α>0, G_1 has only one minimum at D=0

α<0, G_1 acquires two minima at non-zero values of the displacement

Since $E=(\partial G_1/\partial D)_T$ the minima describe the equilibrium values of the spontaneous polarization.

Lines & Glass, Principles and Applications of Ferroelectrics

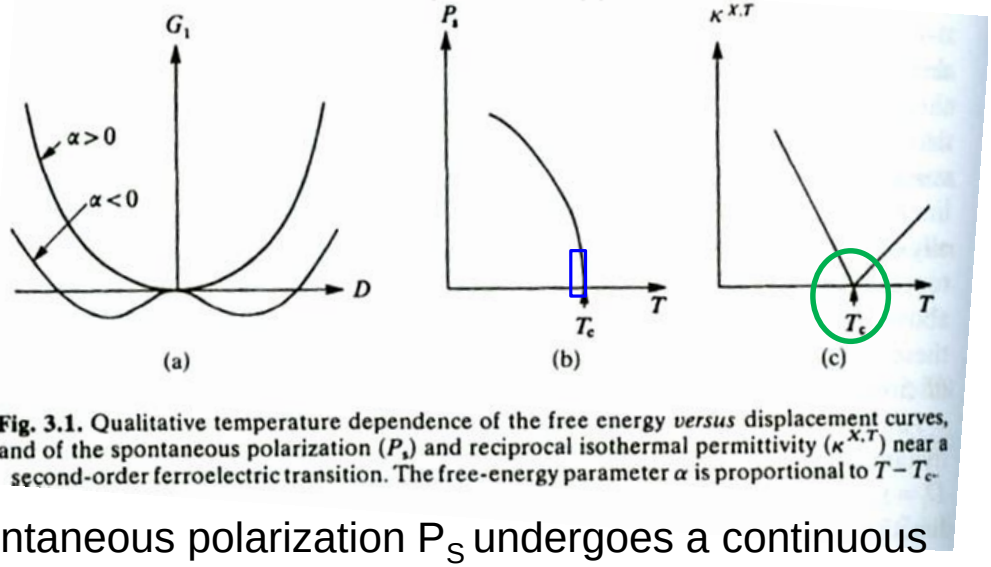

Fig. 3.1. Qualitative temperature dependence of the free energy *versus* displacement curves, and of the spontaneous polarization (P_s) and reciprocal isothermal permittivity ($\kappa^{X,T}$) near a second-order ferroelectric transition. The free-energy parameter α is proportional to $T-T_c$.

Spontaneous polarization P_S undergoes a continuous (second-order) phase transition as α passes through zero and α *has the meaning of* the *reciprocal permittivity at zero-field*, $\alpha = \kappa^{X,T>T_C}$ and is assumed to have the following linear temperature dependence

$\alpha = \beta(T-T_C)$ with β a positive constant

So closely *below* T_C:

$P_S^2 = \beta(T_C-T)/\gamma$, as $P_S \rightarrow 0$

$\kappa^{X,T} = \beta(T-T_C)+3\gamma P_S^2$, as $P_S \rightarrow 0$
so $\kappa^{X,T} = 2\beta(T_C-T)$, $T< T_C$

$LiNbO_3$ (1200°C)
$LiTaO_3$ (620°C)

First-order FE phase transition

A first-order transition point is not a singularity but merely a point at which the thermodynamic potentials of the two phases are equal.

For $\gamma < 0$, $\delta > 0$, and both T-independent:
first-order phase transition
Possible for the potential G_1 to develop equal minima at D=0 and at non-zero values $D = \pm D_C$ ($P = \pm P_C$).

Parameter α is still the reciprocal isothermal permittivity at constant stress in the non-polar phase and Devonshire assumption is again that
$\alpha = \beta (T - T_0)$,
but T_0 is the Curie-Weiss temperature, not equal to the Curie temperature T_C
Writing $\gamma = -\gamma'$, we have
$G_1 = (\beta/2)(T-T_0)D^2 - (\gamma'/4)D^4 + (\delta/6)D^6$

Assuming β, γ' and δ to be positive constants we get the dielectric equation of state

$$E = \beta (T-T_0)D - \gamma' D^3 + \delta D^5$$

Transition takes place at

$$T = T_C = T_0 + (3/16)(\gamma')^2(\beta\delta)^{-1}$$

And at the transition temperature $T=T_C$

$$P_S^2 = P_C^2 = 3\gamma'/4\delta$$

Zero-field permittivity

$$\kappa^{X,T} = 3\gamma'^2/(4\delta) + 8\beta (T_C - T),\ T \rightarrow T_C^-$$

$$\kappa^{X,T} = 3\gamma'^2/(16\delta) + \beta (T_C - T),\ T \rightarrow T_C^+$$

Permittivity is finite but discontinuous at T_C

Lines & Glass, Principles and Applications of Ferroelectrics

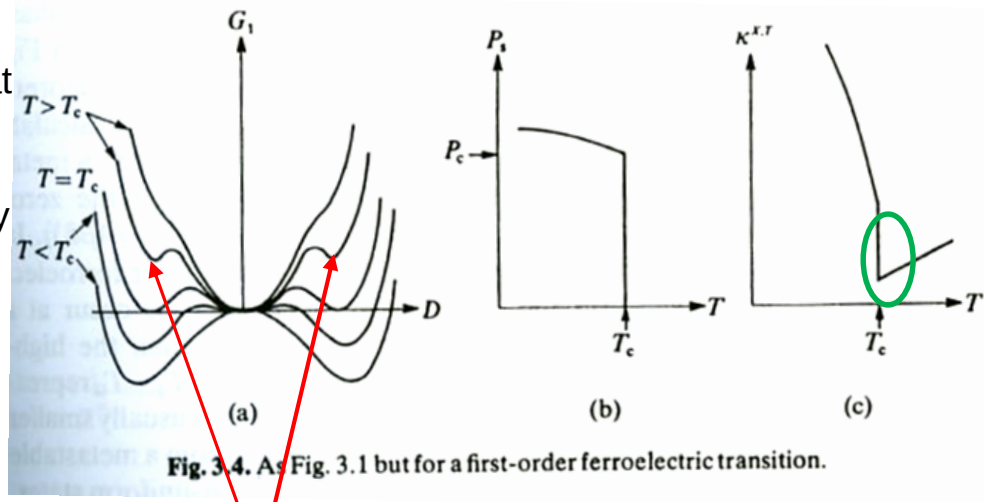

Fig. 3.4. As Fig. 3.1 but for a first-order ferroelectric transition.

The low temperature polar phase can exist at temperatures above T_C as a metastable phase, because a first order PT does not reflect a singularity in thermodynamic potential. And the high-temperature phase can persist below T_C as a metastable phase.
→THERMAL HYSTERESIS EFFECTS

<u>Examples</u>
$BaTiO_3$ (T_C=120°C), all its three PT are 1st order
$PbTiO_3$ (T_C= 493°C)

History (5) : theoretical progress at the MICROscopic level

Simplicity of the perovskite lattice structure allowed theoretical progress at the microscopic level as well:

1950, Slater- *assumed that the ferroelectric behaviour of $BaTiO_3$ was caused by long range dipolar forces that via the Lorentz local effective field tended to destabilize the high symmetry configuration favoured by the local forces*

This explanation became the basic model for DISPLACIVE (as opposed to ORDER-DISORDER) FERROELECTRIC PHASE TRANSITIONS

The concept of ‘rattling‘ titanium became popular when acceptable results were obtained by assuming that one could focus on *the motion of the Ti ion in a rigid framework of the rest of the lattice.*

This approach led to progress:

1960, Andersen and Cochran- *realized that the theory should properly be cast within the framework of lattice dynamics and that one should focus on one of the lattice modes (THE SOFT MODE), involving the ionic motions of all constituent atoms as the basic variable in terms of which to describe the displacive lattice instability.*

Soft phonon (associated with a structural phase transition):
Phonon mode, which coincides with a lower-symmetry structure, and is very much amplified immediately before the onset of phase transition from a higher-symmetry structure.

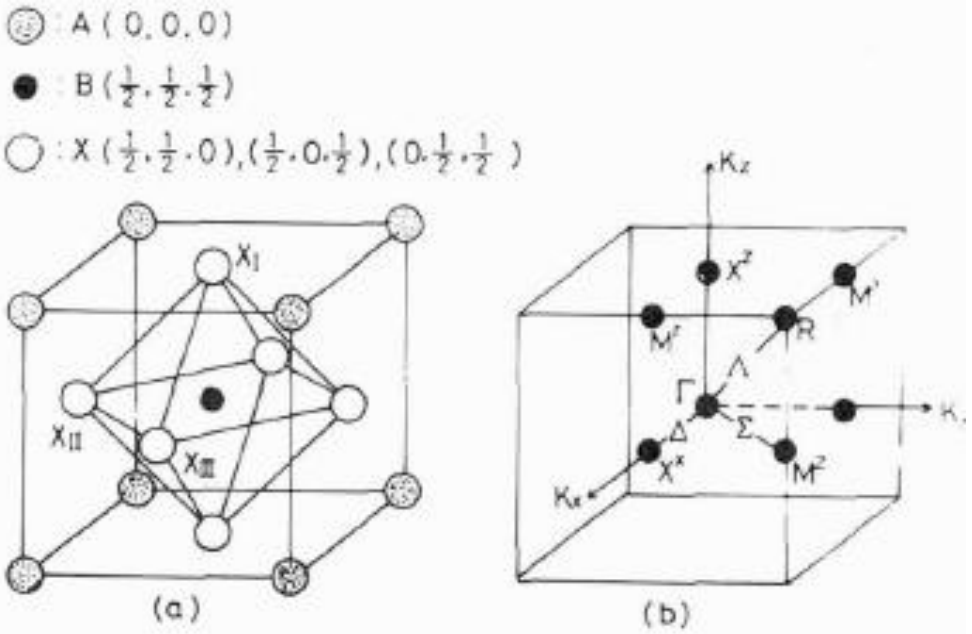

(a) Pervoskite structure and
(b) its Brillouin zone.

Lattice vibration in the perovskite ABX_3 unit cell: mutual vibrations of the 3 sublattices and by displacement modes of the X_6 octahedron
Brillouin zone is a simple cubic lattice and the soft modes are Γ_{15}, M_3 and R_{25}

Displacive phase transitions in $BaTiO_3$

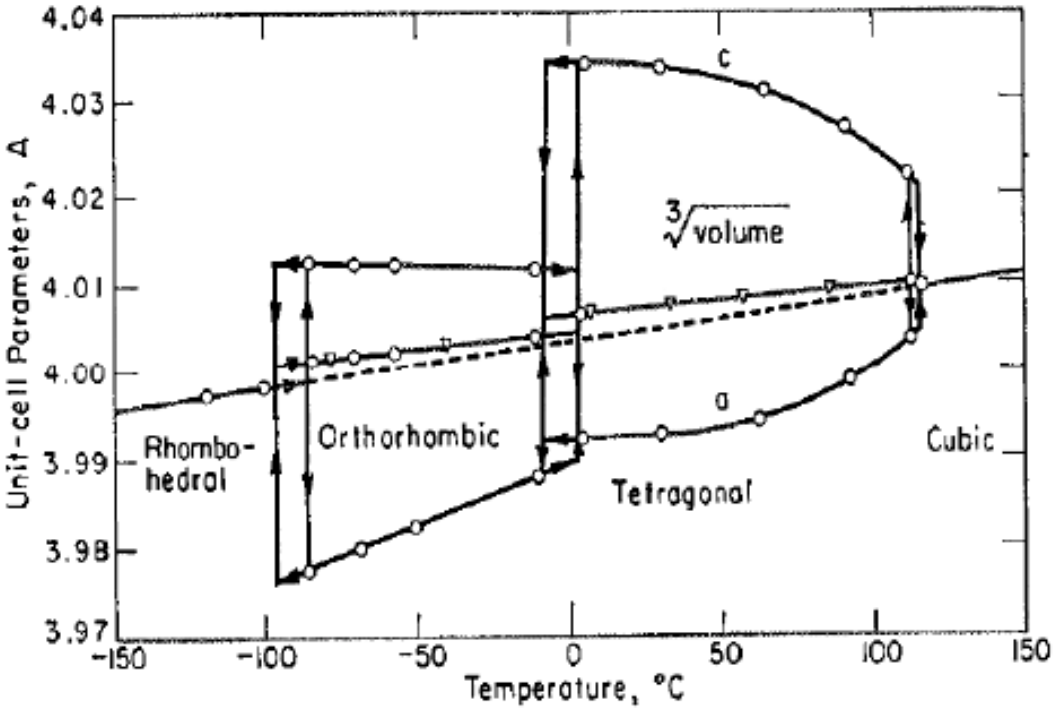

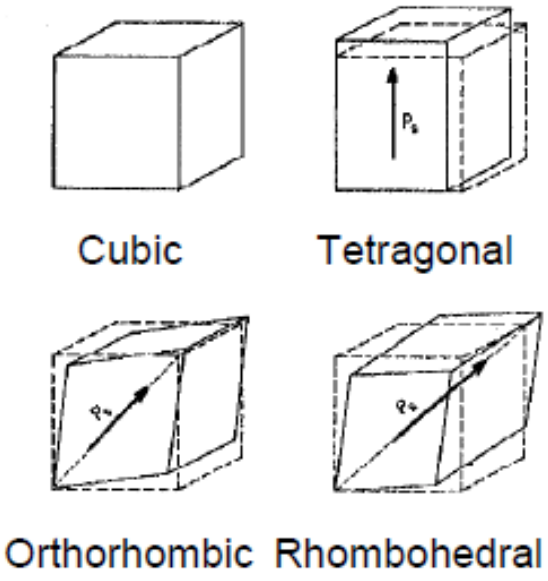

$BaTiO_3$ phase transitions

Condensation of Γ_{15}(optical) mode at the center of the Brillouin zone ($BaTiO_3$)

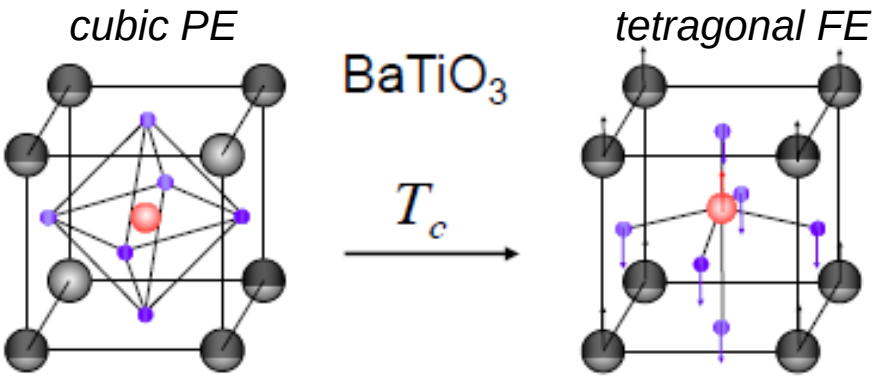

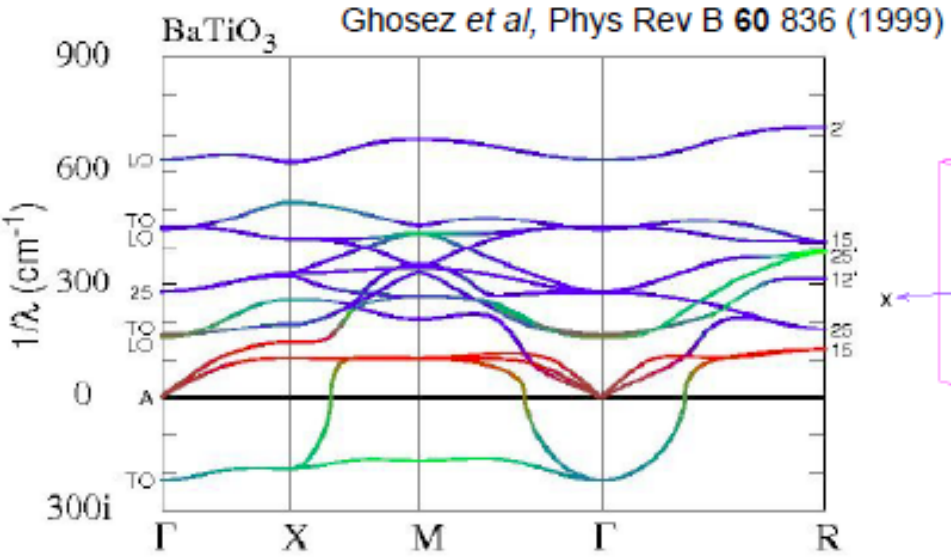

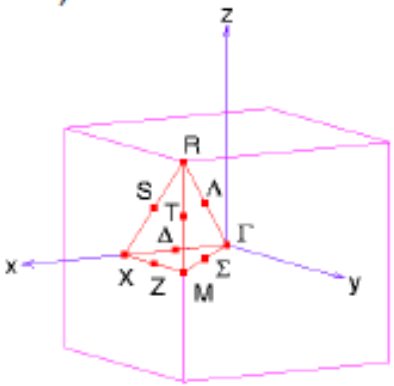

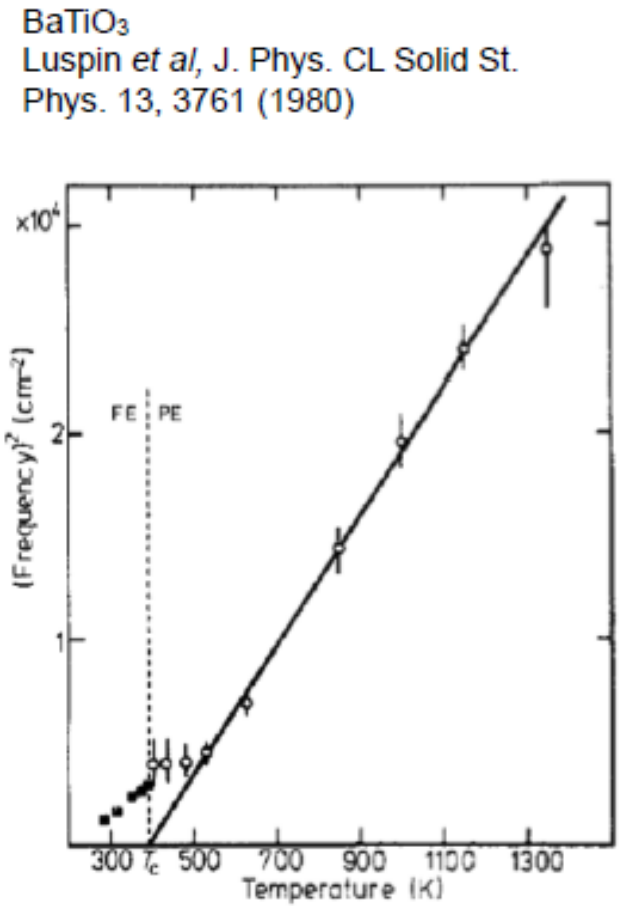

First-principle calculations of phonon dispersions

Physics of Ferroelectrics

A Modern Perspective Karin M. Rabe and Philippe Ghosez

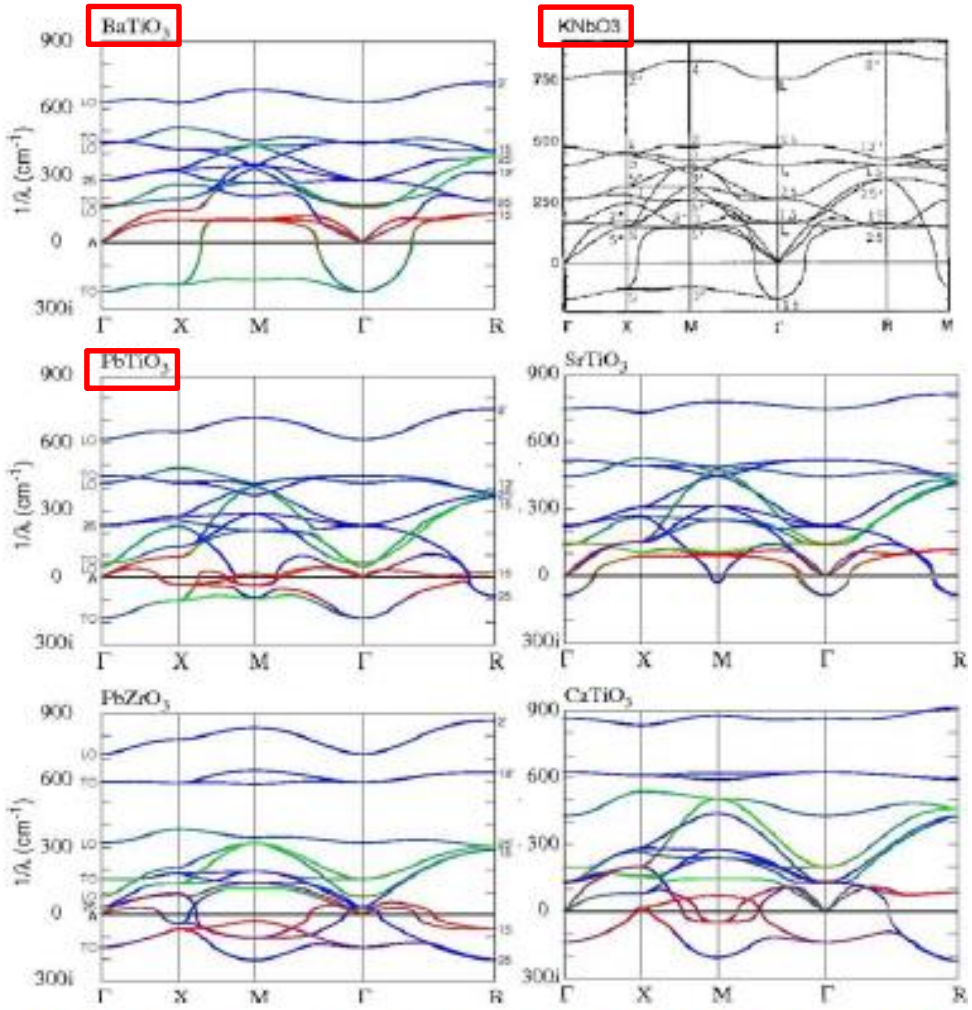

Fig. 3. Phonon dispersions for $BaTiO_3$ [117], $PbTiO_3$ [117], $PbZrO_3$ [117], $KNbO_3$ [151], $SrTiO_3$ [127] and $CaTiO_3$ [163], in the ideal cubic perovskite structure at the experimental lattice constant. Symmetry labels follow the convention of [166], with the A atom at the origin.

Phonons of cubic $BaTiO_3$ (Ghosez thesis)

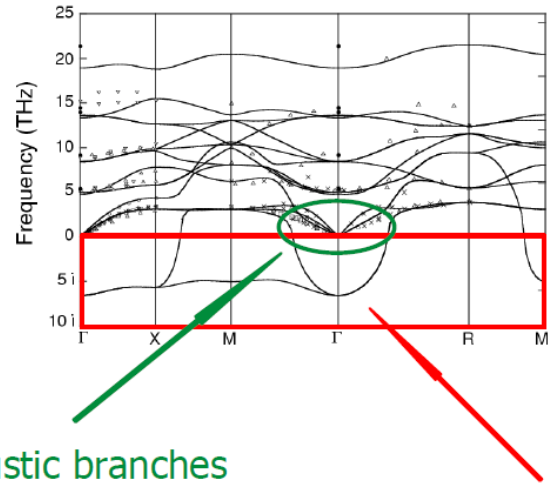

In $BaTiO_3$, the unstable mode is dominated by the Ti displacement and the Ba 5*p* states do not hydridize significantly with the valence band.

In $PbTiO_3$, the Pb participates in the polar distortion and Pb 6*s* "lone-pair" states hybridize with the oxygen 2*p* states.

Similar considerations apply to the behavior of $KNbO_3$: the alkali-metal cation does not participate in the distortion, and the ground-state structure resembles that of $BaTiO_3$.

Modern theory of ferroelectric perovskites

Origin of ferroelectricity in perovskite oxides

NATURE · VOL 358 · 9 JULY 1992

Ronald E. Cohen
Geophysical Laboratory, Carnegie Institution of Washington, 5251 Broad Branch Road NW, Washington DC 20015, USA

FERROELECTRIC materials are characterized by a switchable macroscopic polarization. Most technologically important ferroelectrics are oxides with a perovskite structure. The origin of their ferroelectric behaviour is unclear, however, and there is incomplete understanding of why similar, but chemically different, perovskites should display very different ferroelectric behaviour. The great sensitivity of ferroelectrics to chemistry, defects, electrical boundary conditions and pressure arises from a delicate balance between long-range Coulomb forces (which favour the ferroelectric state) and short-range repulsions (which favour the nonpolar cubic structure). To model the transition accurately, total-energy techniques are required which incorporate the effects of charge distortion and covalency. Here I report results of electronic-structure calculations on two classic examples of ferroelectric perovskites, $BaTiO_3$ and $PbTiO_3$, and demonstrate that hybridization between the titanium 3*d* states and the oxygen 2*p* states is essential for ferroelectricity. The different ferroelectric phase behaviour of the two materials is also clear: in $PbTiO_3$, the lead and oxygen states hybridize, leading to a large strain that stabilizes the tetragonal phase, whereas in $BaTiO_3$ the interaction between barium and oxygen is completely ionic, favouring a rhombohedral structure.

Modern theory of ferroelectrics applied to perovskite titanates

FIG. 1 Calculated energy as a function of soft-mode distortion in (*a*) $PbTiO_3$ and (*b*) $BaTiO_3$. The $PbTiO_3$ wells are much deeper than for $BaTiO_3$. In both $BaTiO_3$ and $PbTiO_3$ without strain the rhombohedral phase has lower energy. In $PbTiO_3$, however, tetragonal strain stabilizes the tetragonal phase over the rhombohedral phase. In $BaTiO_3$ strain has a much smaller effect and the rhombohedral phase is still lower in energy. The large volume effect (pressure decreases the well depths) is more obvious in $BaTiO_3$ because of the smaller energy scale.

Energy as a function of soft-mode distorsio

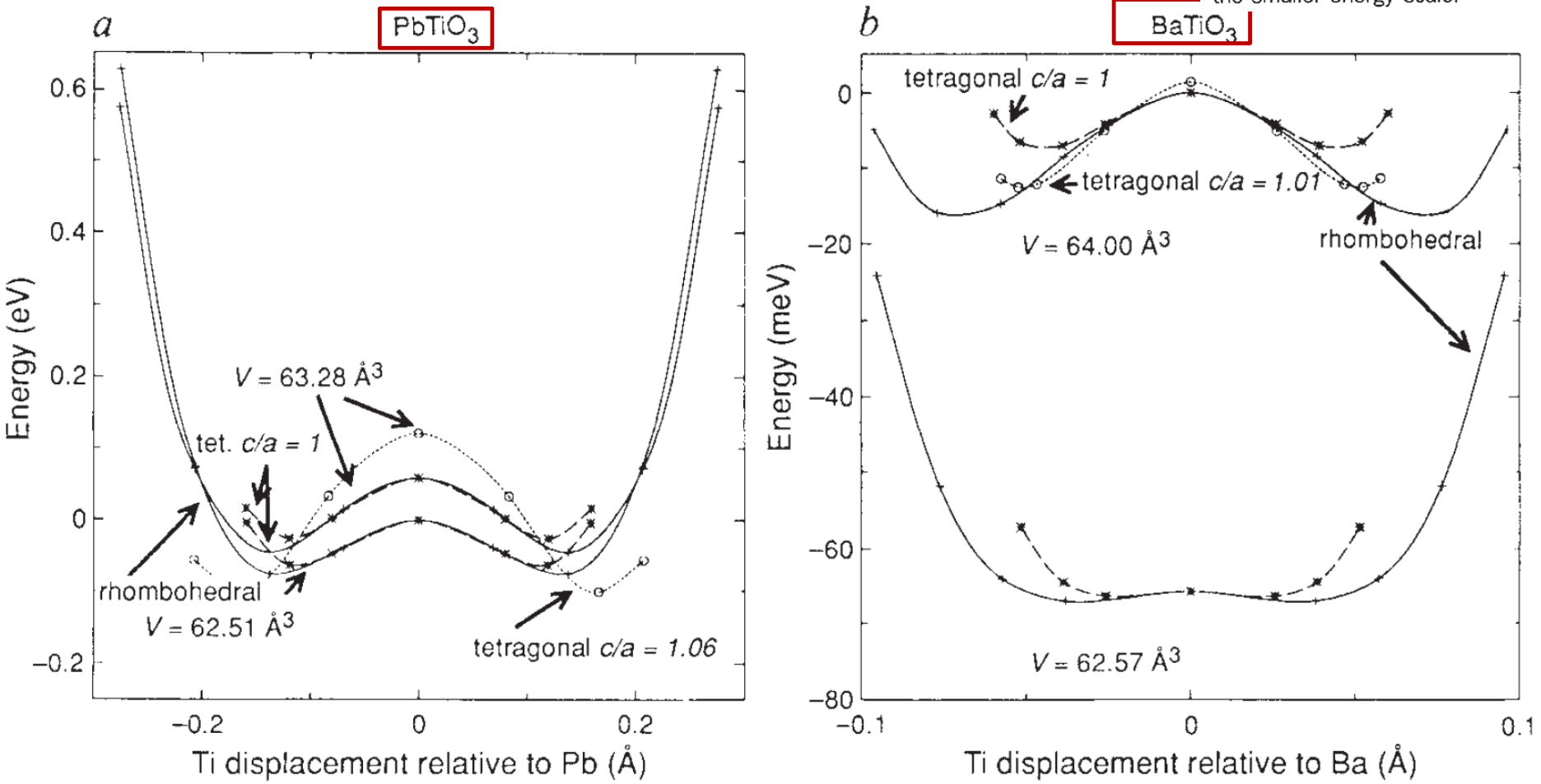

Modern theory of ferroelectrics applied to perovskite titanates

FIG. 2 Electronic density of states against energy relative to the valence-band maxima for (*a*) ferroelectric $PbTiO_3$ (horizontal stripes) and cubic $PbTiO_3$ (vertical stripes), and (*b*) ferroelectric $PbTiO_3$ (horizontal) and $BaTiO_3$ (vertical stripes). The top panels show the total densities of states and the bottom two show the contributions (partial densities of states) from the regions around the Ti for states with *d* character and around Pb or Ba with *s* or *p* character, respectively. Overlap of the Ti 3*d* and Pb 6*s* partial densities of states with the primarily oxygen 2*p* valence bands, which range from 0 to ~ −5.5 eV, indicates considerable hybridization. The ferroelectric distortion also lowers the eigenvalue sum, helping to decrease the total energy. The $PbTiO_3$ structure was used for $BaTiO_3$ to obtain the results in the right panels (*b*) so that the differences are due solely to the replacement of Pb by Ba; whereas the Pb *s* state is strongly hybridized with the oxygen 2*p* states, the Ba is fully ionic. The Ti–O interactions are also different in $BaTiO_3$ and $PbTiO_3$ even with the same structure, because they are influenced in the latter by the Pb–O interaction.

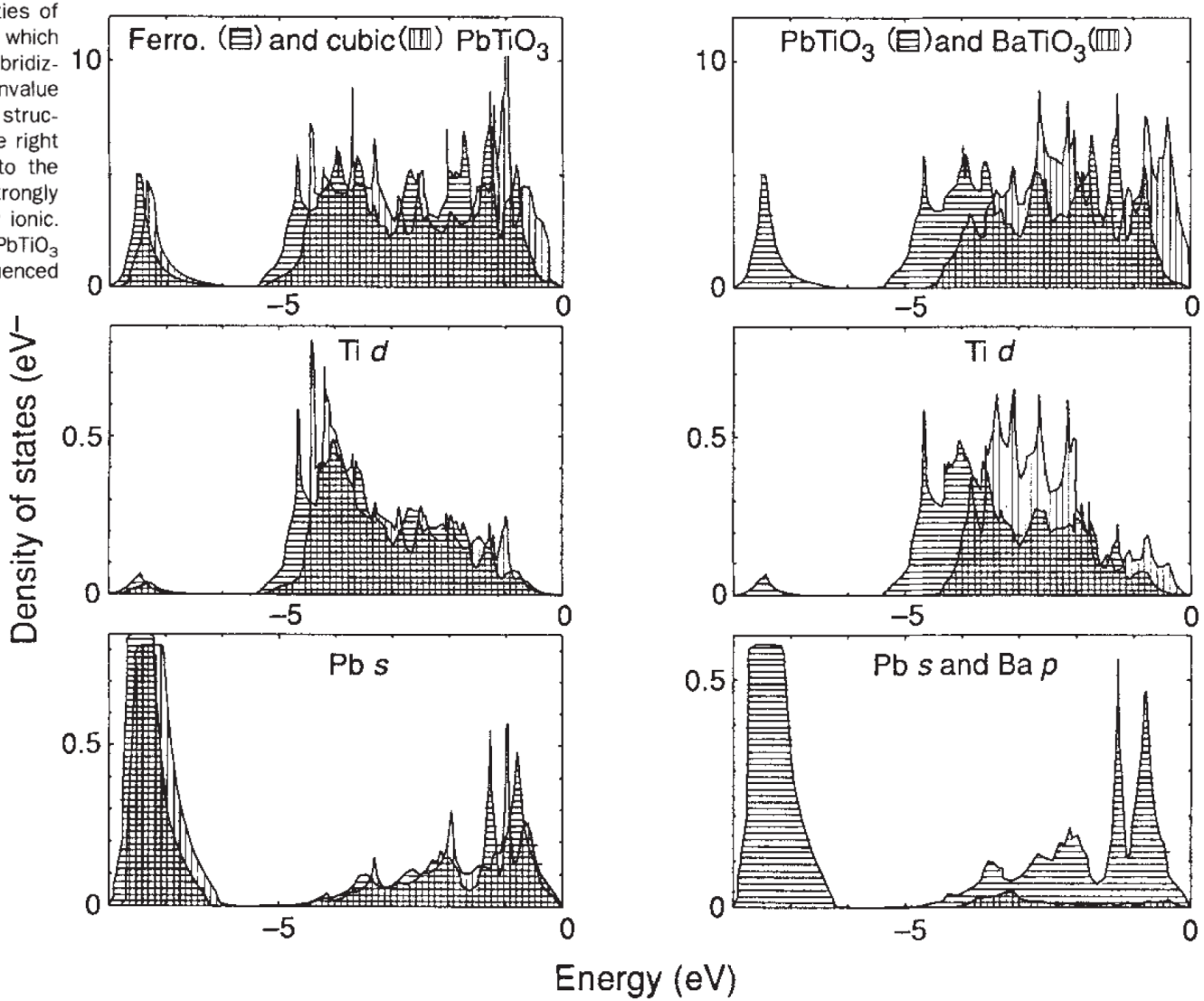

Modern theory of ferroelectrics applied to perovskite titanates

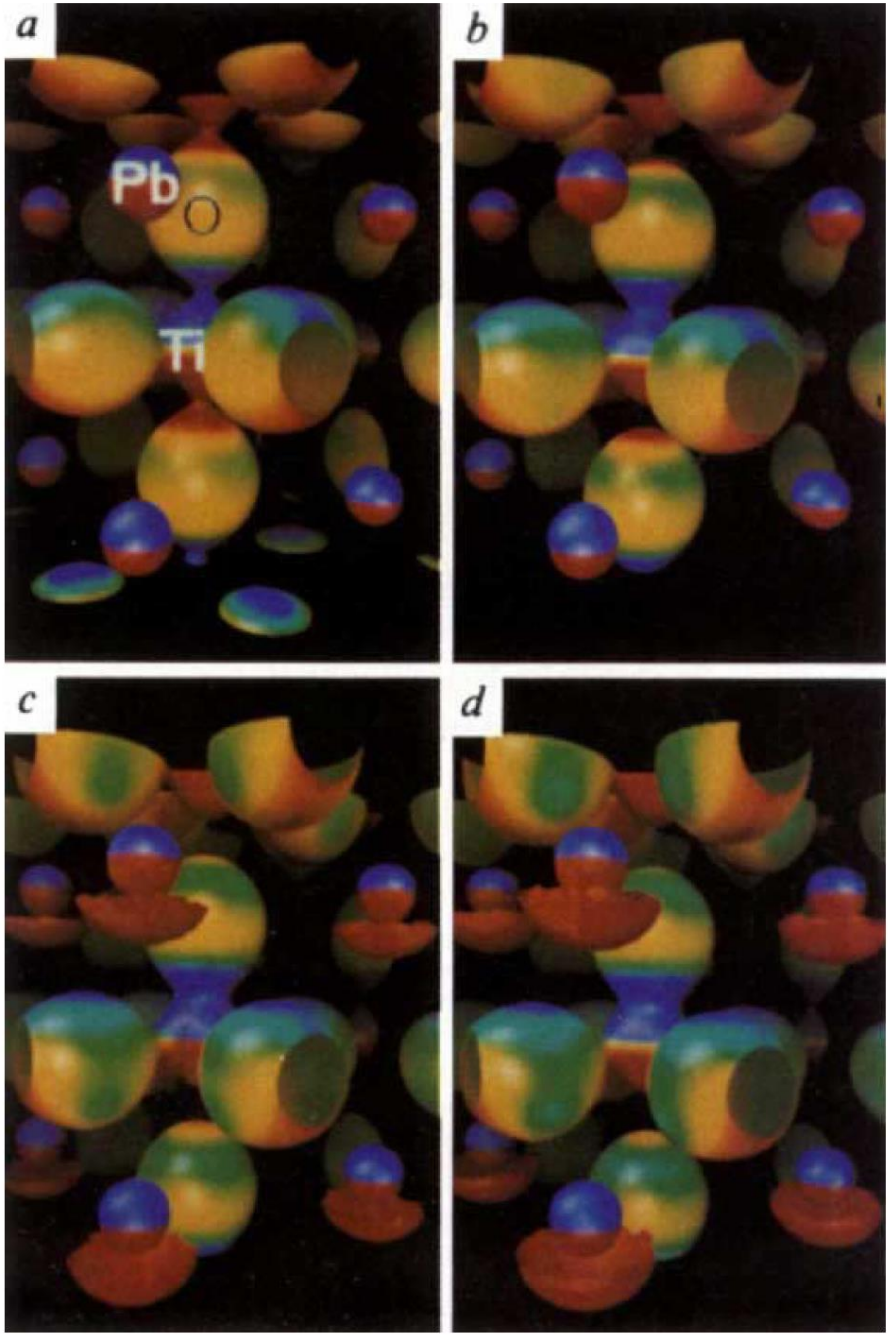

FIG. 3 Valence charge density of $PbTiO_3$ for increasing ferroelectric distortions (all with $c/a=1.06$). The O and Ti atoms are displaced towards the bottom of the figure. Panels *a*–*d* correspond to the four strained tetragonal points in Fig. 1*a*. Constant density surfaces for 0.26 electrons $Å^{-3}$ are shown. The charge density corresponds to the oxygen 2*p* bands as well as the Pb *s* band. The most important features are the significant valence charge density on the Ti (Ti^{4+} would have essentially no valence charge) and the clear polarization of the Pb ions. A similar distortion does not occur around the Ba in $BaTiO_3$. The colours give the *z*-component of the electric field at each point on the surface. Near the nuclei the electric field is dominated by the nuclear field, but at greater distances the asymmetry between the red and blue colouring indicates the periodic field that forms in the crystal because of the ferroelectric distortion. A finite crystal could also develop a macroscopic field, depending on the surface boundary conditions.

The bonding has a mixed ionic/covalent character in typical ferroelectric oxides, with a sizeable fraction of the electronic charge shared among ions in a delocalized manner→ fallacy of the Clausius-Mossotti (classic ionic) picture and relation, which assumes that the charge distribution of a polarized solid system is given by the superposition of localized contributions, each providing an electric dipole.

Electric-field induced (pseudo)charge density

Ionic NaCl crystal: extreme ionic case

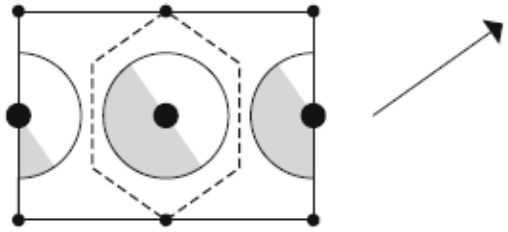

Fig. 1. A polarized ionic crystal having the NaCl structure, as represented within an extreme Clausius–Mossotti model. We qualitatively sketch the electronic polarization charge (*shaded areas indicate negative regions*) in the $(1\bar{1}0)$ plane linearly induced by a constant field $\boldsymbol{\mathcal{E}}$ in the [111] direction as indicated by the arrow. The anions (*large circles*) are assumed to be polarizable, while the cations (*small circles*) are not. The boundary of a Wigner–Seitz cell, centered at the anion, is also shown (*dashed line*)

Silicon crystal: extreme covalent case

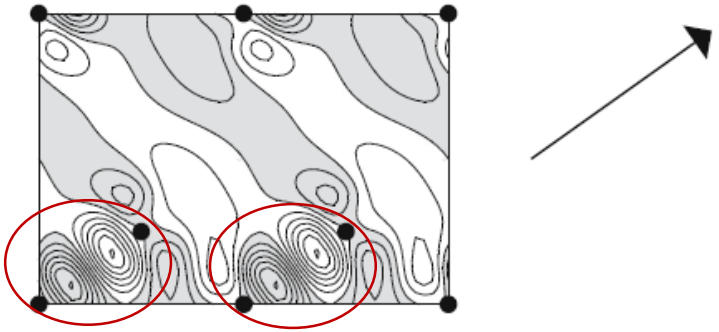

Fig. 2. Induced (pseudo)charge density $\rho^{(\mathrm{ind})}(\boldsymbol{r})$ in the $(1\bar{1}0)$ plane linearly induced by a constant field $\boldsymbol{\mathcal{E}}$ in the [111] direction, indicated by the arrow, in crystalline silicon. The field has unit magnitude (in a.u.) and the contours are separated by 30 charge units per cell. Shaded areas indicate regions of negative charge; circles indicate atomic positions

How is induced/spontaneous polarization measured?

1. By using the direct piezoelectric effect in piezoelectrics/ ferroelectrics

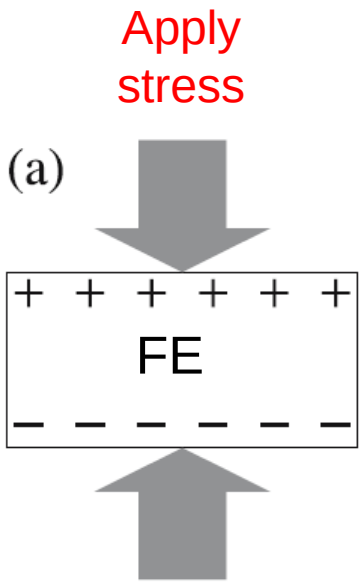

Open-circuit
Charges pile up on the surfaces of the FE crystal upon stress application

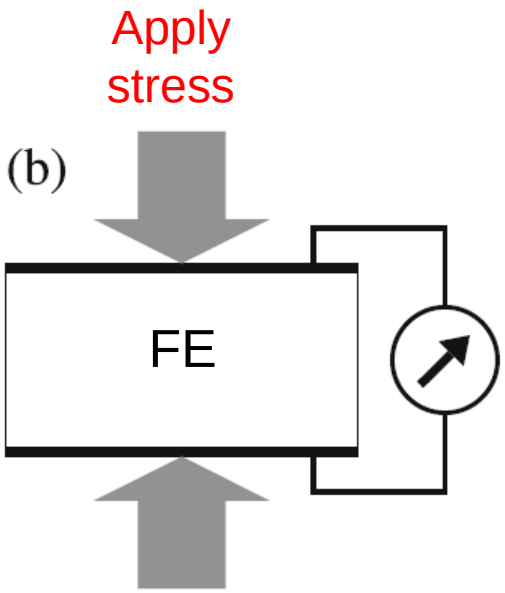

Short-circuit
The FE crystal is inserted into a shorted capacitor; the surface charges are then being removed by the electrodes, and the induced polarization is measured by the current flowing through the wires.

$$\frac{\mathrm{d}\boldsymbol{P}(t)}{\mathrm{d}t} = \boldsymbol{j}(t)\,, \quad \Delta\boldsymbol{P} = \boldsymbol{P}(\Delta t) - \boldsymbol{P}(0) = \int_0^{\Delta t} \mathrm{d}t\, \boldsymbol{j}(t)$$

Notice that, in the adiabatic limit, ***j*** goes to zero and Δ*t* goes to infinity, while the integral stays finite. Also currents are much easier to measure than dipoles or charges, and therefore (b), much more than (a), is representative of actual piezoelectric measurements.

How is induced/spontaneous polarization measured?

2. By using the electrically switchable character of FE spontaneous polarization

Positive-Up-Negative-Down (PUND) method

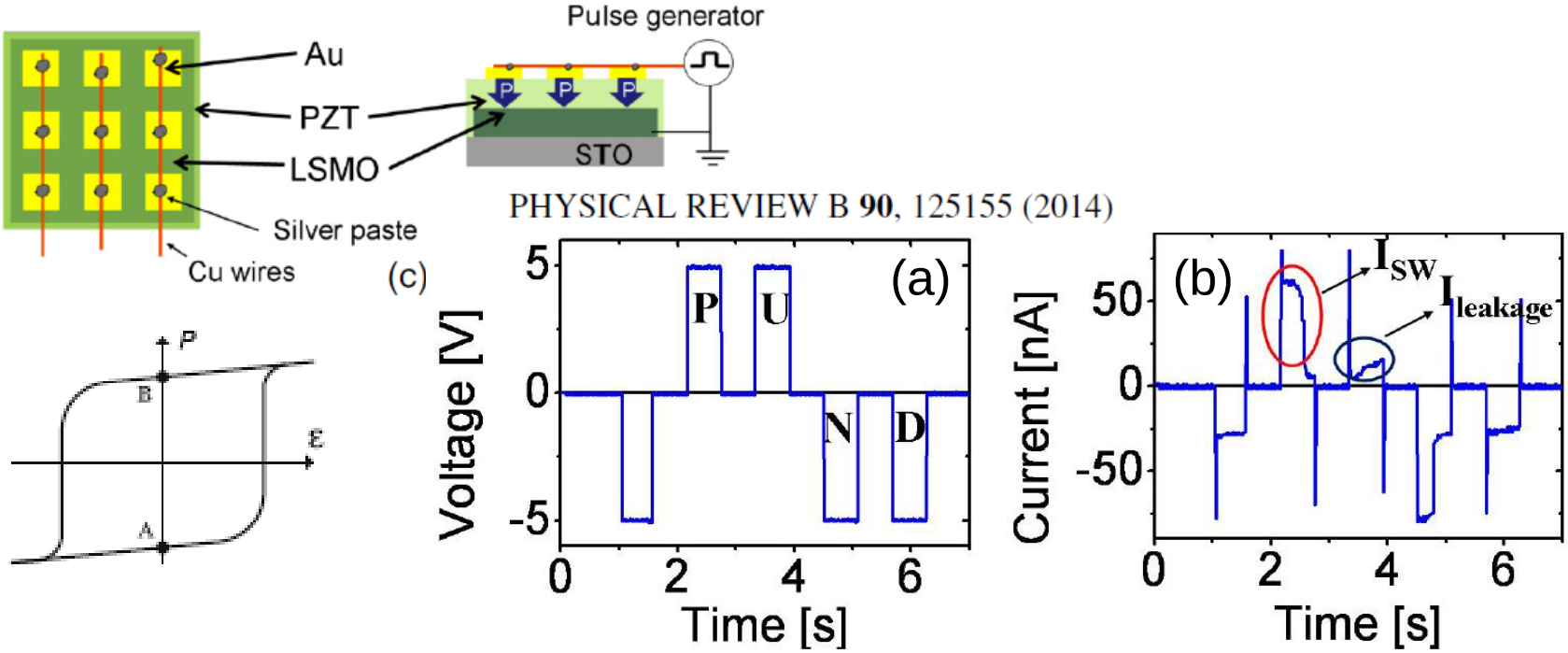

Measured current is given in (b): the difference between the current obtained during the P pulse (indicated in red) and the U pulse (indicated in blue) is very clear. The leakage current (due to the electronic transport across the ferroelectric layer) is visible while applying the U pulse. Similar behavior can be inferred from the subsequent N and D pulses. By integration over time of the obtained free-leakage current peak (i.e. U(D)-P(N)), normalized to the total electrode area and averaged between both voltage polarities, a total amount of switchable polarization is obtained.The experiment measures neither P_A(down state) nor P_B (up state) but their difference and it is only an additional symmetry argument that allows one to infer the value of each of them from the actual experimental data.

Theory of polarization: a modern approach

The role of adiabatic currents in measuring the induced and spontaneous polarization suggests a new approch in dealing with the microscopic theory of polarization, which must be an intensive bulk property, insensitive to the boundary conditions.

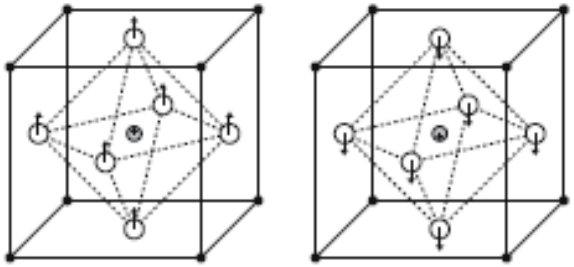

λ - a dimensionless adiabatic time: λ varies continuously from 0 (corresponding to the initial system) to 1 (corresponding to the final system).
In order to focus the discussion onto the spontaneous polarization of a FE, we now let λ scale the sublattice displacements (the lengths of the arrows in the figure), leading from a centrosymmetric reference structure ($\lambda = 0$) to the spontaneously polarized structure ($\lambda = 1$).
The spontaneous polarization may be written as the integral:

Effective polarization: $$\boldsymbol{P}_{\text{eff}} = \int_0^1 \mathrm{d}\lambda \, \frac{\mathrm{d}\boldsymbol{P}}{\mathrm{d}\lambda} \qquad (\lambda = 0 : \text{centrosymmetric reference})$$

→ BERRY-PHASE theory of polarization (developed in the 1990th) can yield the “formal“ polarization

Berry-phase theory of polarization (formulation in continuous *k*- space)

For a crystalline system, the self consistent potential has the lattice periodicity; the eigenfunctions are of the Bloch form

$$\psi_{n\boldsymbol{k}}(\boldsymbol{r}) = \mathrm{e}^{\mathrm{i}\boldsymbol{k}\cdot\boldsymbol{r}}\, u_{n\boldsymbol{k}}(\boldsymbol{r}), \text{ where } u \text{ is lattice-periodical}$$

And obey the Schrödinger equation.

$$H|\psi_{n\boldsymbol{k}}\rangle = E_{n\boldsymbol{k}}\,|\psi_{n\boldsymbol{k}}\rangle \qquad H_{\boldsymbol{k}} = \frac{(\boldsymbol{p}+\hbar\boldsymbol{k})^2}{2m} + V\,.$$

All these quantities depend on λ that varies continuously but slowly in time and the time t in the current density j= d**P**/dt can be eliminated by replacing d**P**/dt →d**P**/dλ .

Fourier transform

Berry phase

Berry connection

Atomic position

$$P = \frac{e}{(2\pi)^3}\,\Im\sum_n \int \mathrm{d}\boldsymbol{k}\,\langle u_{n\boldsymbol{k}}|\nabla_{\boldsymbol{k}}|u_{n\boldsymbol{k}}\rangle + \frac{e}{\Omega}\sum_s Z_s^{\mathrm{ion}}\,\boldsymbol{r}_s$$

electronic contribution

ionic contribution

This result is independent of the path traversed through parameter space and of the rate of traversal, as long as it is adiabatically slow, so that the result depends only on the end points!
Implicit is that the system must remain insulating everywhere along the path, otherwise the adiabatic condition fails.

Ferroelectric Random Access Memory cell – Principal idea

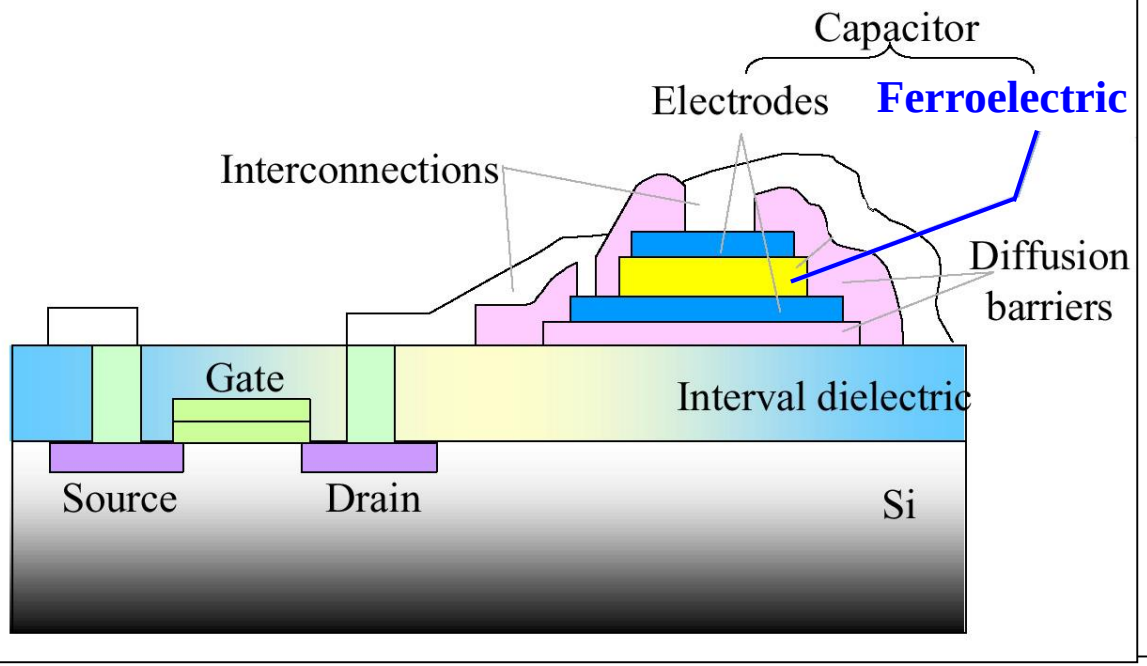

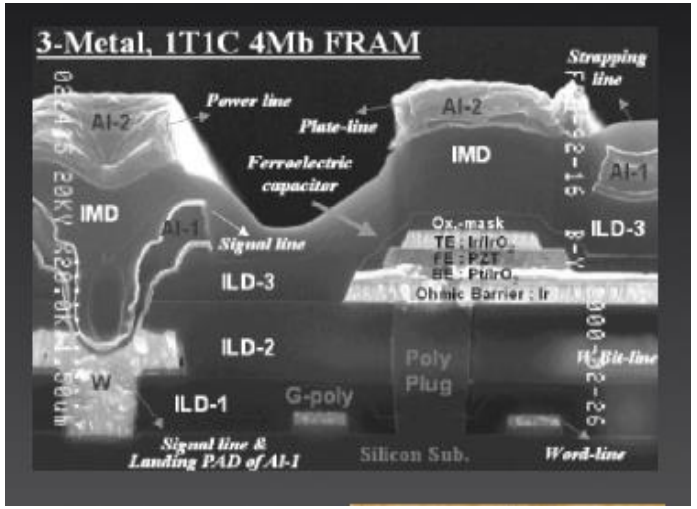

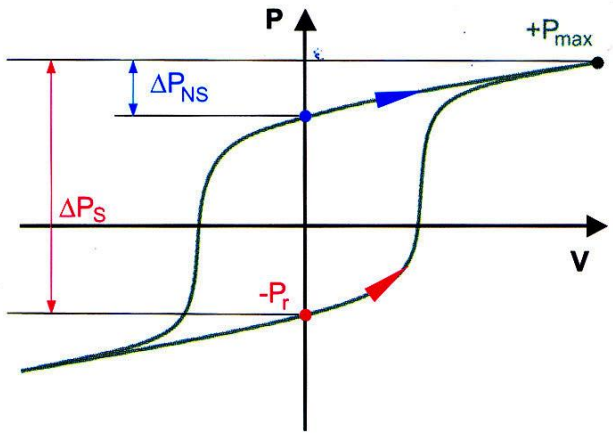

Figure 1: Non-switching and switching of the polarization of a ferroelectric capacitor

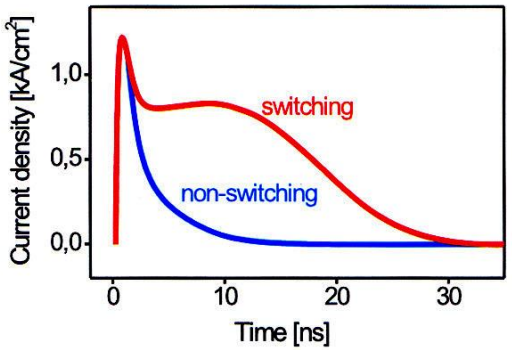

Figure 2: Current response of non-switching and switching case of the ferroelectric polarization.

Waser, 2003

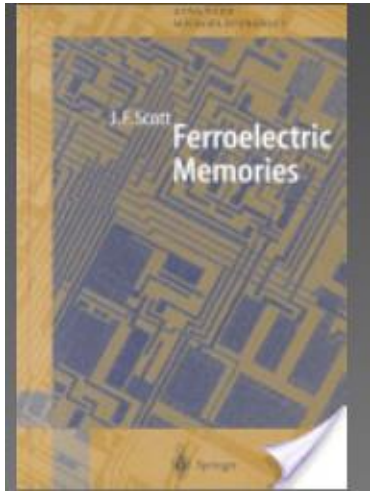

*MULTI*FERROICS

Ferroic order parametrs

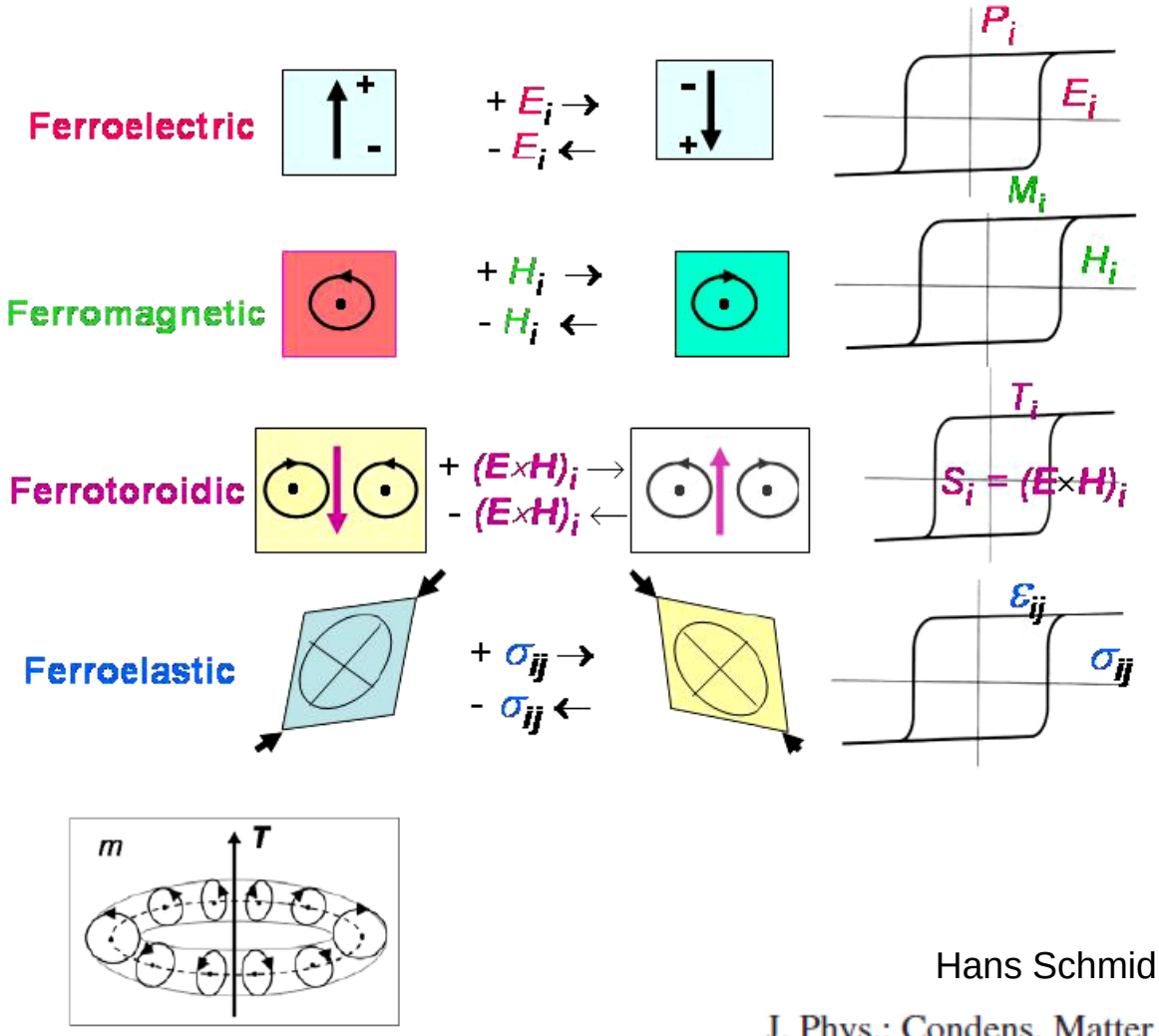

Hans Schmid

J. Phys.: Condens. Matter **20** (2008) 434201

Figure 1. Schematic domain switching and hysteresis cycles of the four primary ferroics. The symmetry symbol used for the toroidal moment corresponds to the co-axial mirror plane cross-section of a toroid with an even number of windings (see inset). Note that for certain symmetries, a toroidal moment cannot only be switched by $(E \times H)_i$, but also by collinear electric and magnetic fields or by a magnetic field alone (cf section 3.2.2).

Ferroelectric/ferroelastic domains

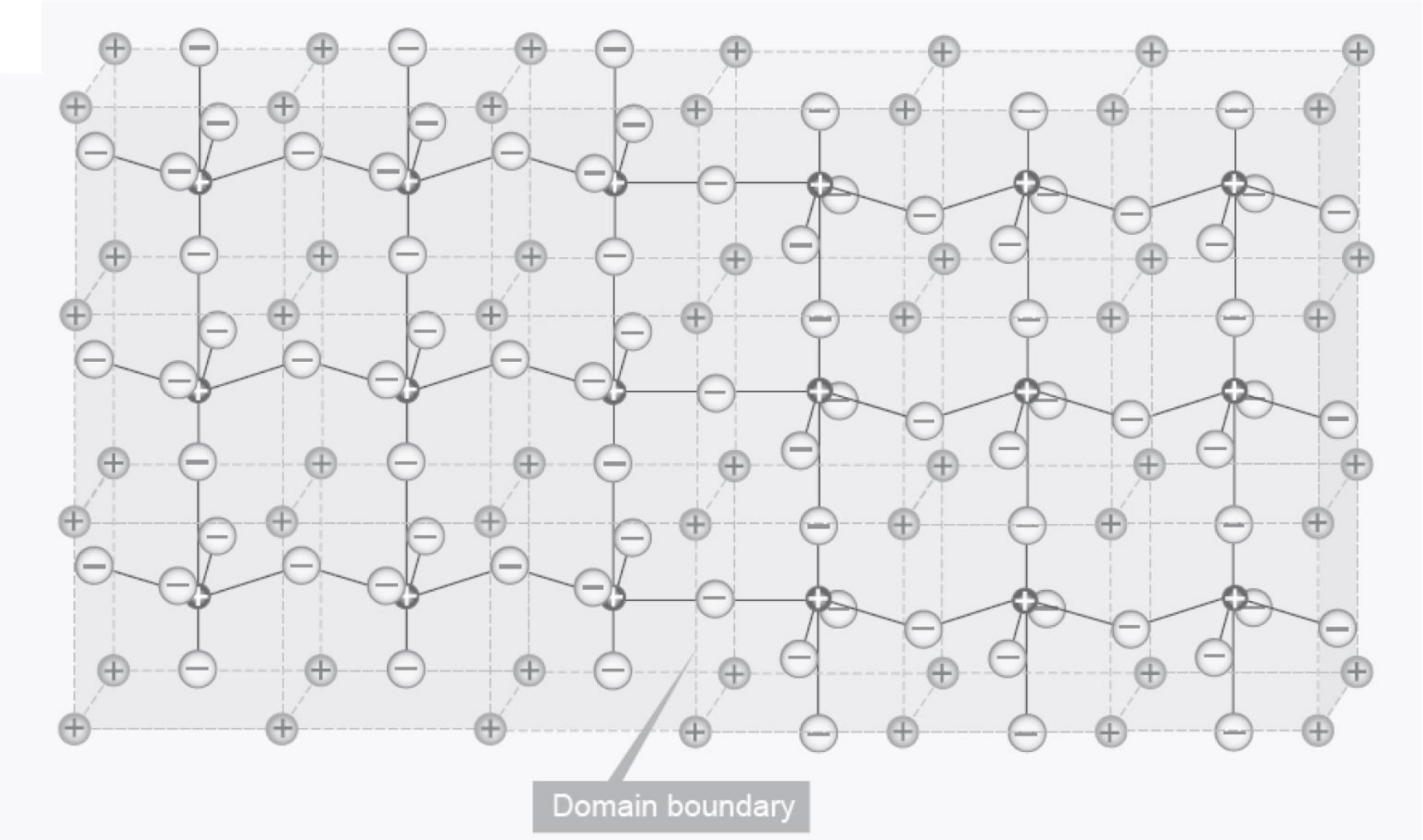

Figure 1.2: *Schematic representation of a 180º domain wall in $PbTiO_3$. [11]*

Karin M. Rabe, Charles H. Ahn, Jean-Marc Triscone Eds., Physics of Ferroelectrics. A Modern Perspective, Topics Appl. Physics 105 (2007)

Ferroelectric/ferroelastic domains

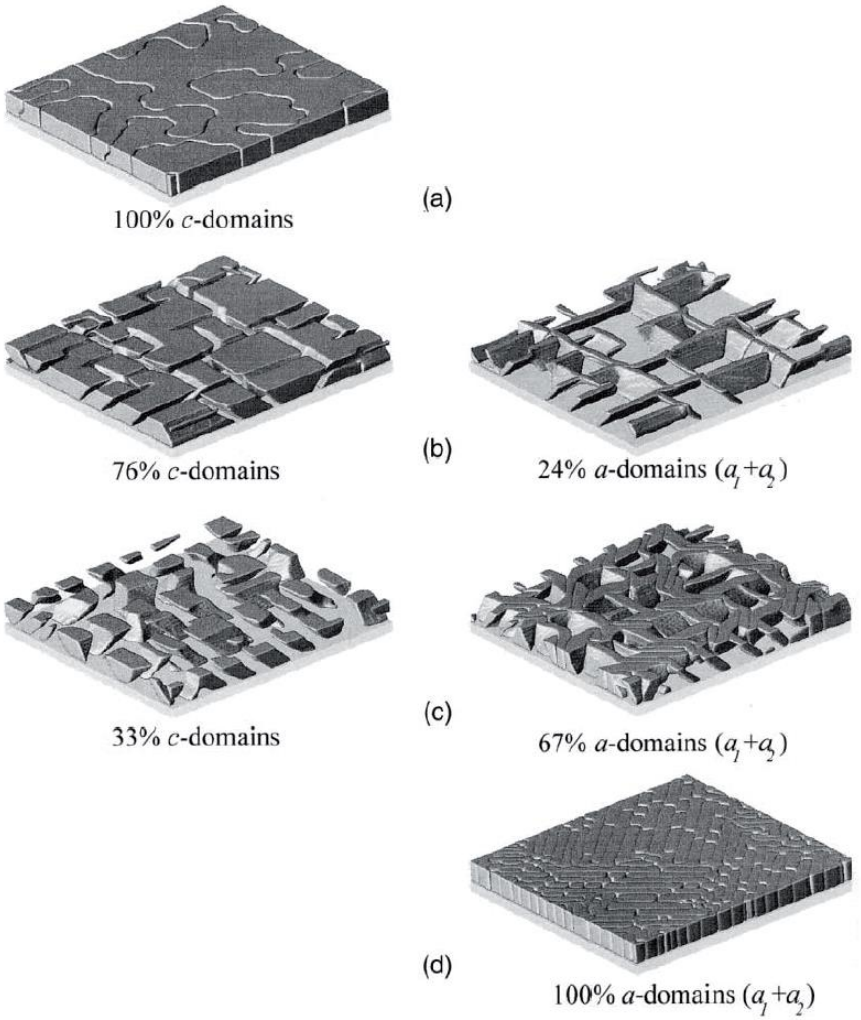

Figure 1.7: *Domain structures calculated for a $PbTiO_3$ film obtained from phase field simulations. a) c-domains. b) $c/a_1/a_2$ domain structure with 76% of c-domains. c) $c/a_1/a_2$ domain structure with 33% of c-domains. d) a_1/a_2 domain structure [45]*

Karin M. Rabe, Charles H. Ahn, Jean-Marc Triscone Eds., Physics of Ferroelectrics. A Modern Perspective, Topics Appl. Physics 105 (2007)

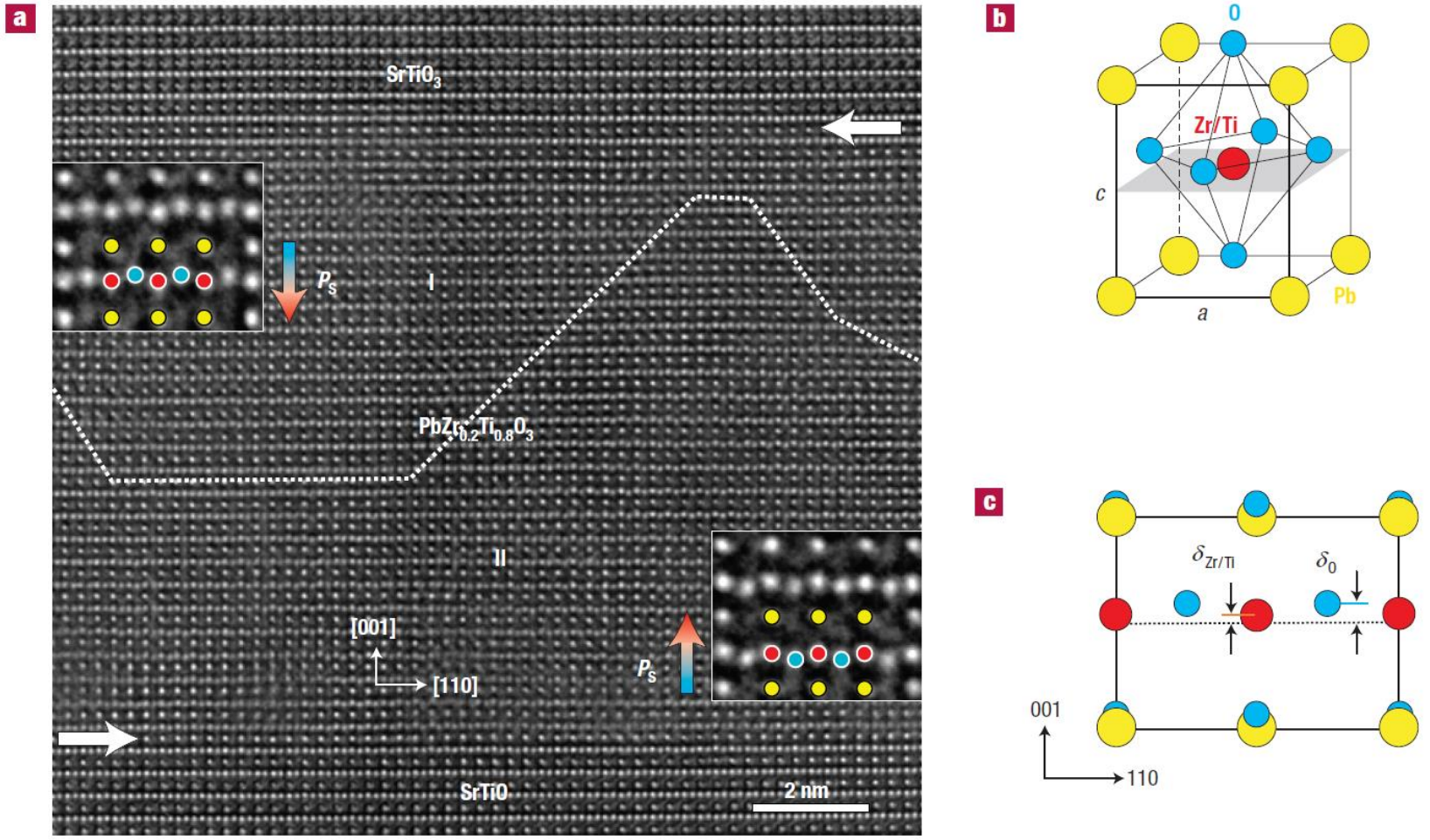

Figure 1 **Atomic-scale imaging of the electric dipoles formed by the relative displacements of the Zr/Ti cation columns and the O anion columns. a**, Image of a $SrTiO_3/PbZr_{0.2}Ti_{0.8}O_3/SrTiO_3$ thin-film heterostructure. The image is recorded under negative spherical-aberration imaging conditions with the incident electron beam parallel to the $[\bar{1}10]$ direction. The atom columns appear bright on a dark background. The horizontal arrows denote the horizontal interfaces between the $PbZr_{0.2}Ti_{0.8}O_3$ and the top and the bottom $SrTiO_3$ film layers. The dotted line traces the 180° domain wall. The arrows denoted by 'P_S' show the directions of the polarization in the 180° domains. The insets show magnifications of the dipoles formed by the displacements of ions in the unit cells (yellow: PbO, red: Zr/Ti, blue: O). **b**, Schematic perspective view of the unit cell of ferroelectric $PbZr_{0.2}Ti_{0.8}O_3$. **c**, Projection of the unit cell along the $[\bar{1}10]$ direction. $\delta_{Zr/Ti}$ and δ_O denote the shifts of the Zr/Ti atoms and the oxygen atoms, respectively, from the centrosymmetric positions.

CL Jia, K. Urban, I. Vrejoiu et al, Nature Materials 2008

Polarization-Magnetization coupling possible?

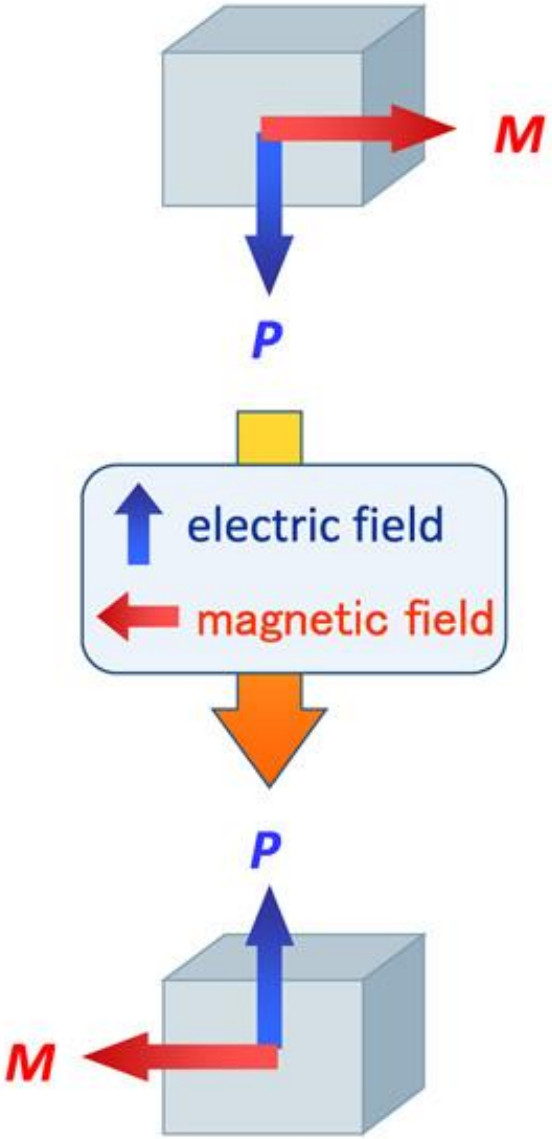

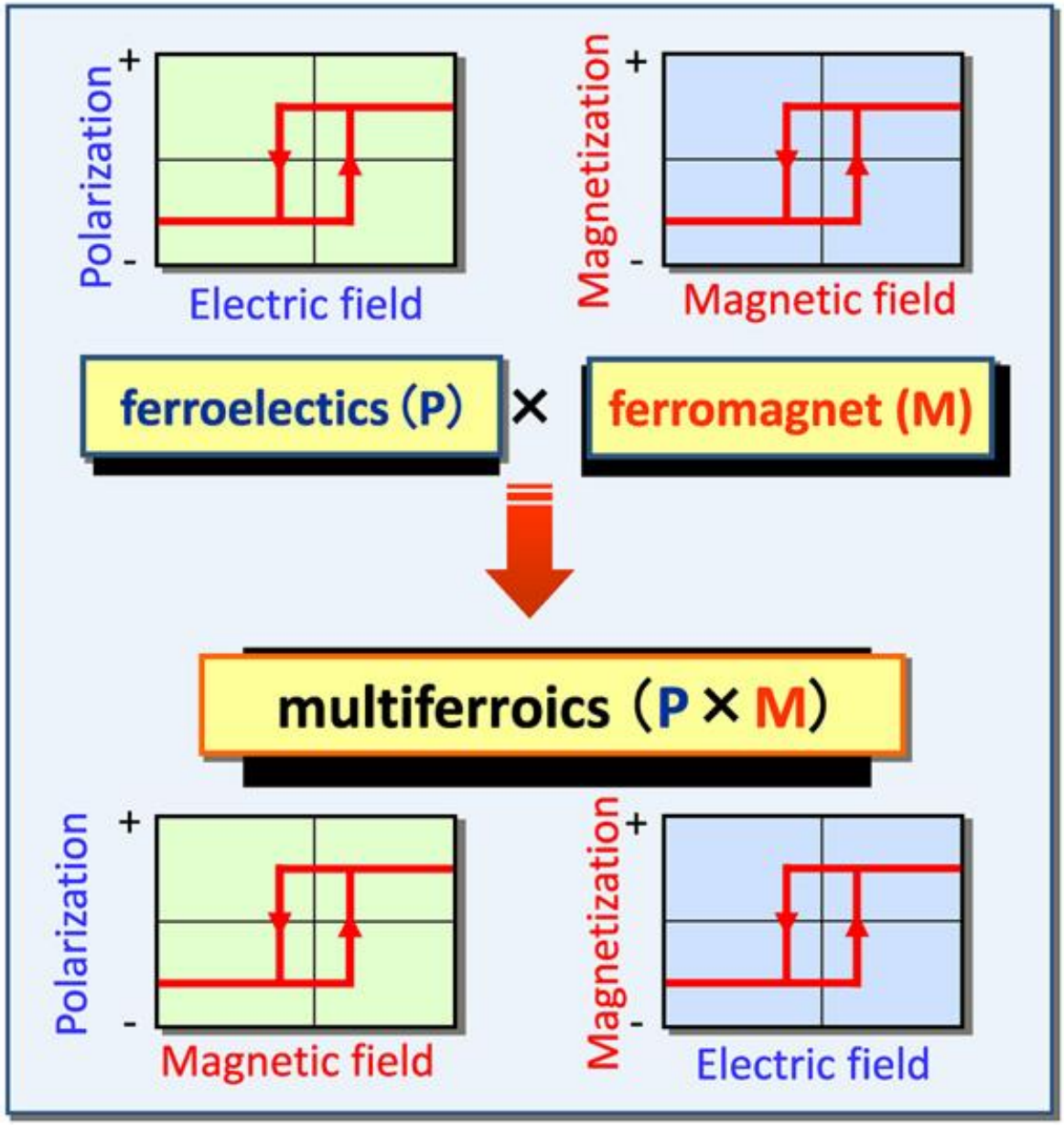

Lone-pair active ferroelectrics: an approach towards perovskite oxide, ABO_3, multiferroic materials

Chemical incompatibility between magnetism and conventional ferroelectricity is related to the fact that the most common mechanism for ferroelectricity in perovskite-structure oxides involves the presence of a transition metal cation on the perovskite B site with a formal d^0 electron configuration. For magnetism to occur in such transition metal oxides a partially filled *d* shell is indispensable.

C. Ederer and N. A. Spaldin, Current Opinion in Solid State and Mater. Sci., 2005

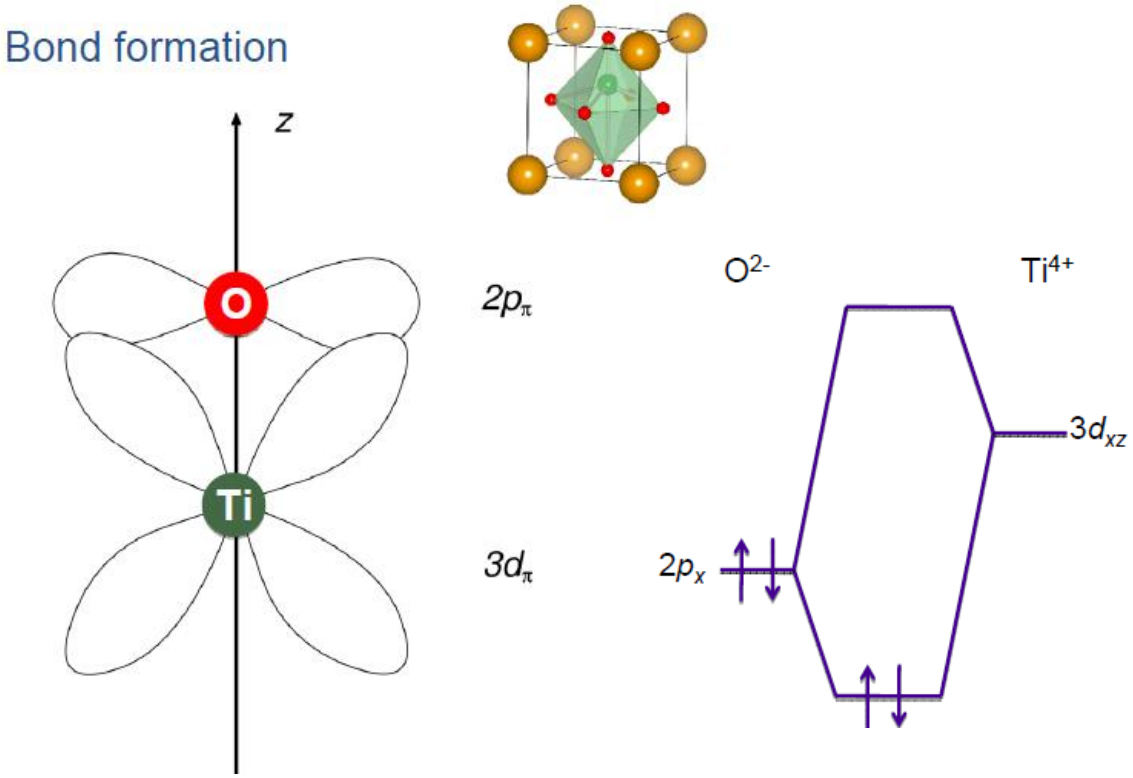

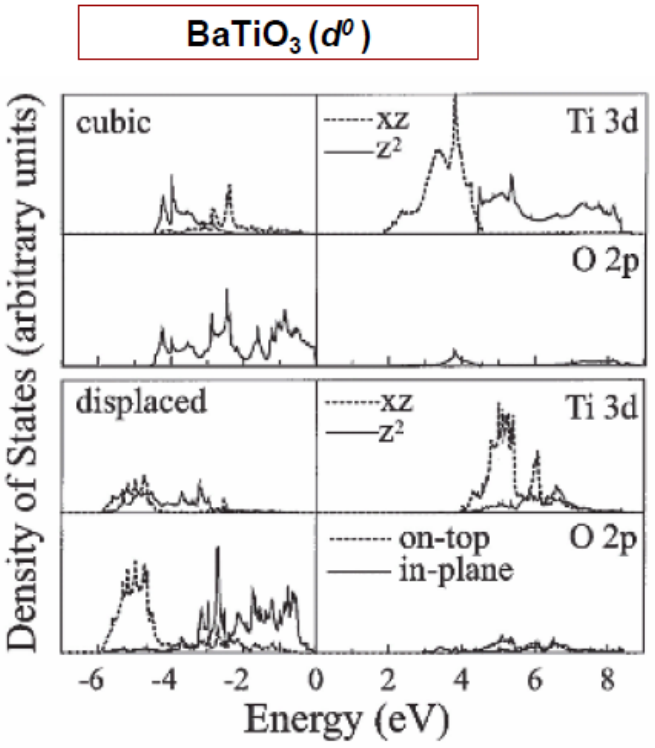

A. Filippetti and N.A. Hill, PRB **65**, 195120 (2002).

Lone-pair active ferroelectrics: an approach towards perovskite oxide, ABO_3, multiferroic materials

Magnetism from a 3d transition metal (Mn^{3+})

Examples: $BiFeO_3$, $BiMnO_3$

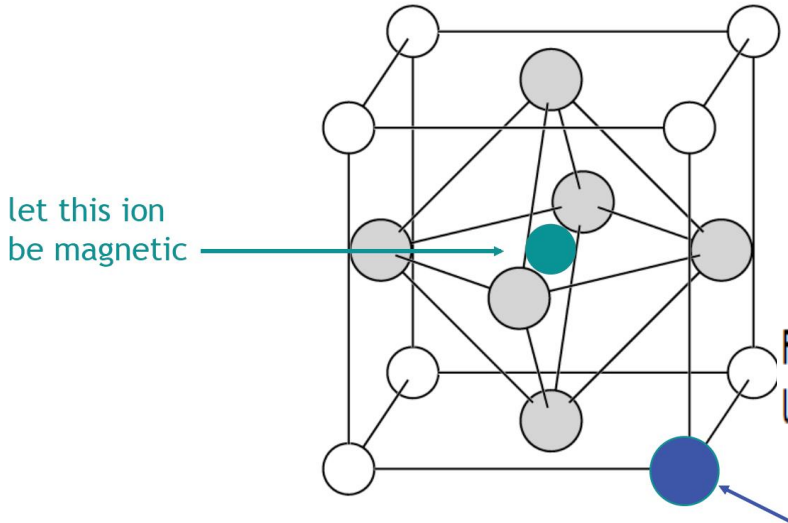

Ferroelectricity from the "stereochemically active lone pair" on Bi^{3+} (cf ammonia, NH_3)

7 N: $2s^2\ 2p^3$

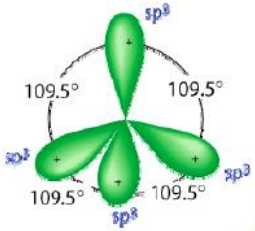

NH_3 molecule →

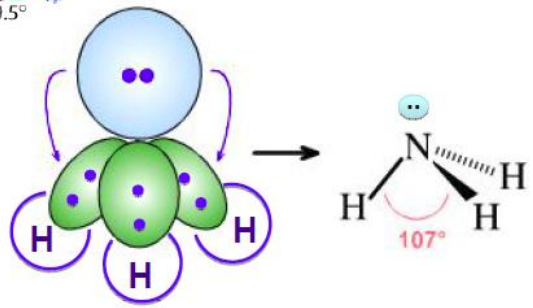

$BiFeO_3$

Ferroelectric (T_C= 1100 K) with record polarization, $P_{[111]}$= 95 μC/cm^2, and **antiferromagnetic** (T_N= 640 K) with canted spins (weak ferromagnetic)→ **intrinsically multiferroic at RT**!

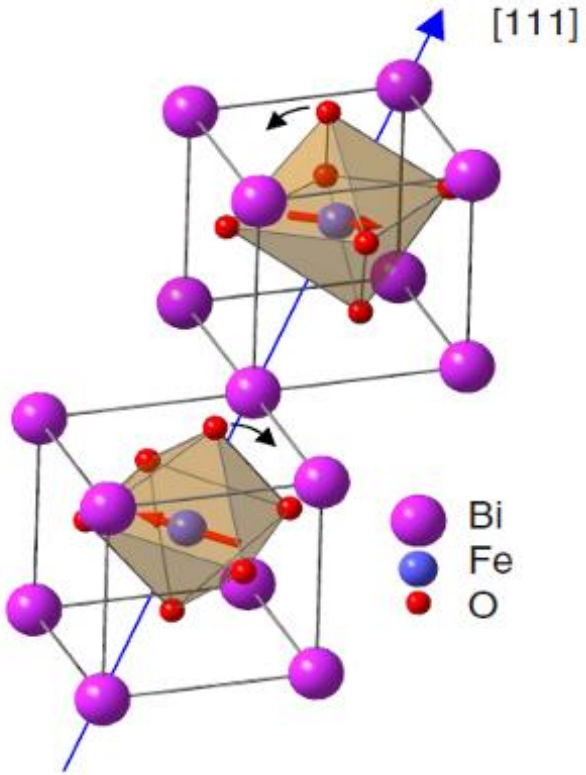

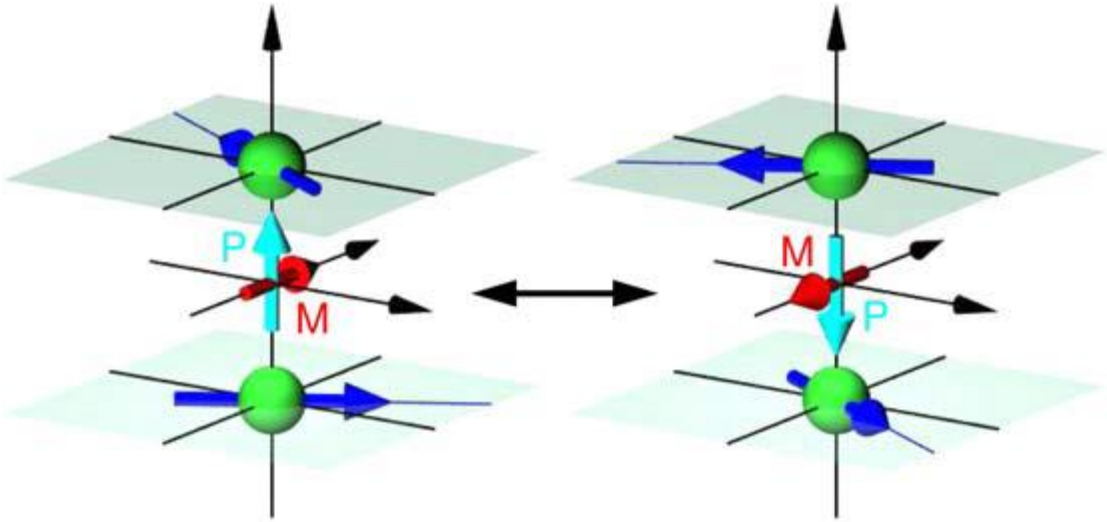

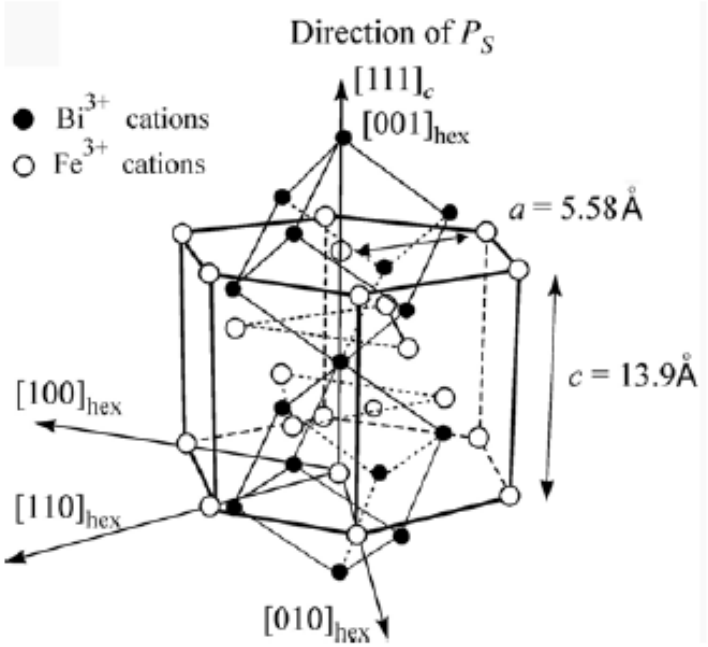

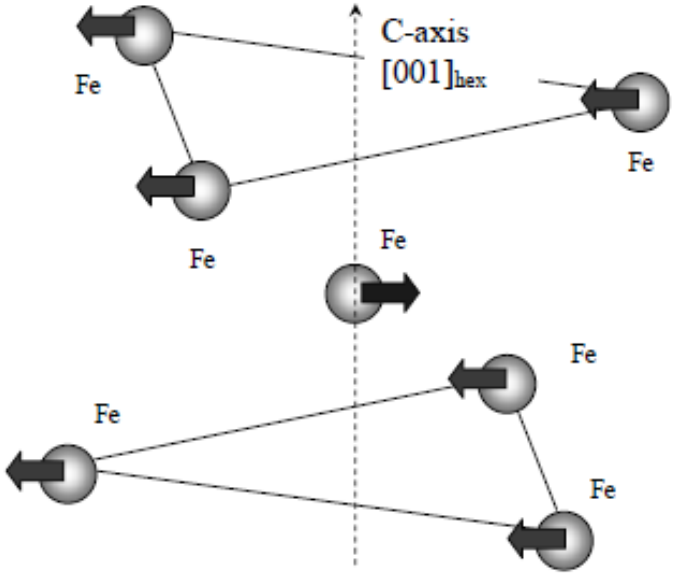

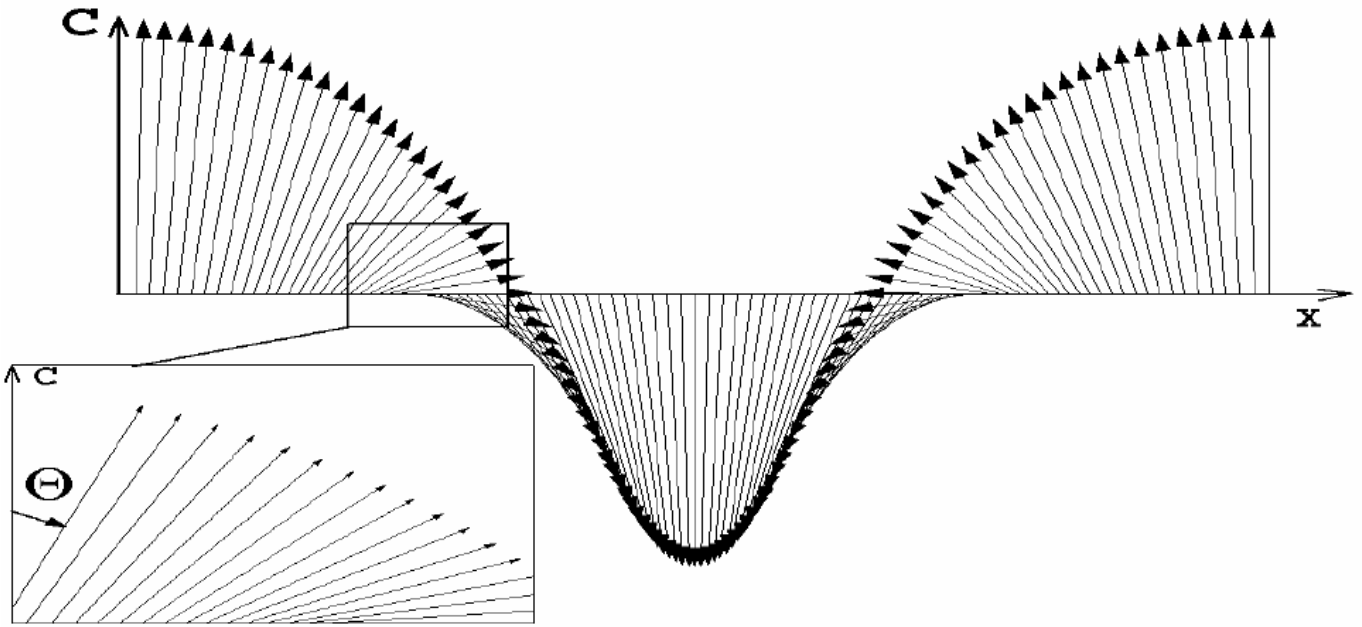

Fig. 2 Long range magnetic order: incommensurate spin cycloid. The arrows correspond to the antiferromagnetic vector L that changes its orientation in space $\theta = \theta(x)$.

Preferred domain patterns

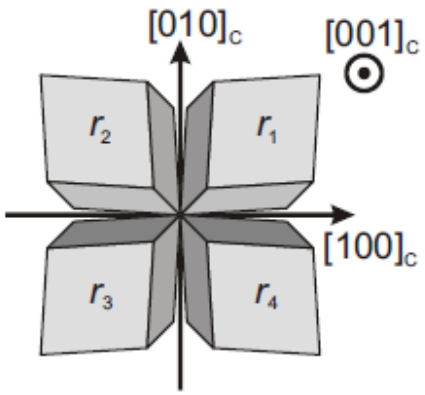

- minimizing mechanical and electrical energy

→ mechanical and charge compatibility at domain wall

- for rhombohedral ferroelectrics: Streiffer, JAP 83, 2742 (1998)

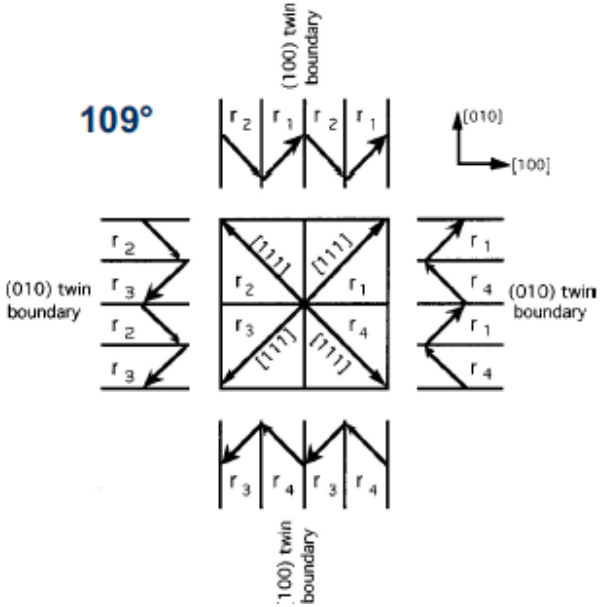

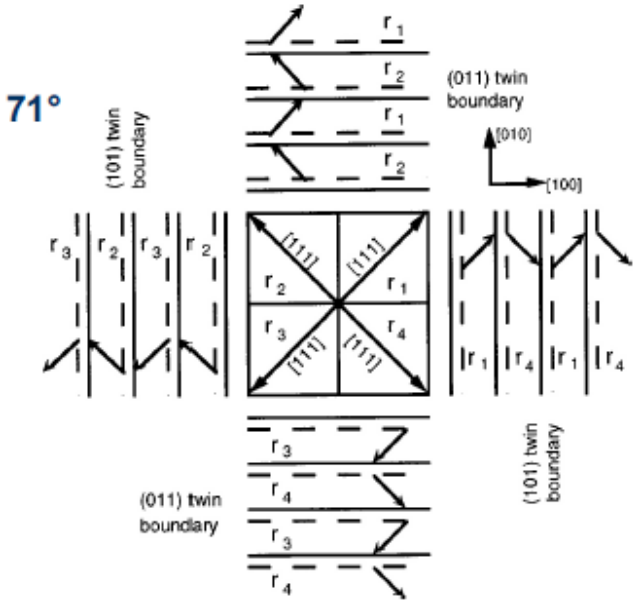

F. Johann, MPI Halle

Piezoresponse Force Microscopy (PFM)

Visualization of ferroelectric domains

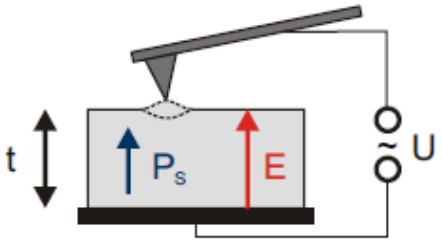

- Ferroelectricity ⇒ Piezoelectricity:
  $\Delta t = d \cdot E \cdot t = d \cdot U$
  (d: piezoelectric coefficient [pm/V])
- AFM tip as top electrode
- AC voltage for filtering with Lock-In

→ Opposite domains have 180° phase shift

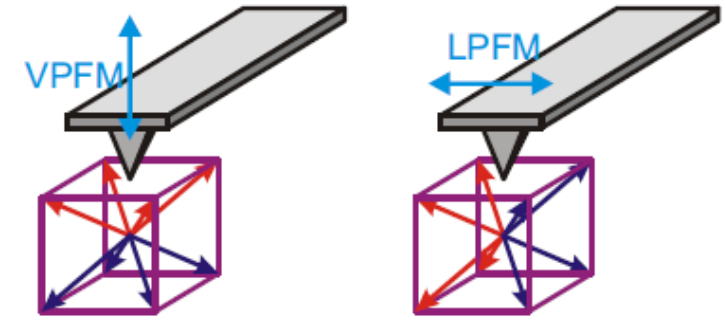

Vertical PFM Lateral PFM

PFM on BFO:

VPFM: out-of-plane projection

LPFM: in-plane projection perpendicular to cantilever

F. Johann, MPI Halle

Extrinsic magneto-electric coupling between two layers: ferromagnetic CoFe and antiferromagnetic ferroelectric $BiFeO_3$

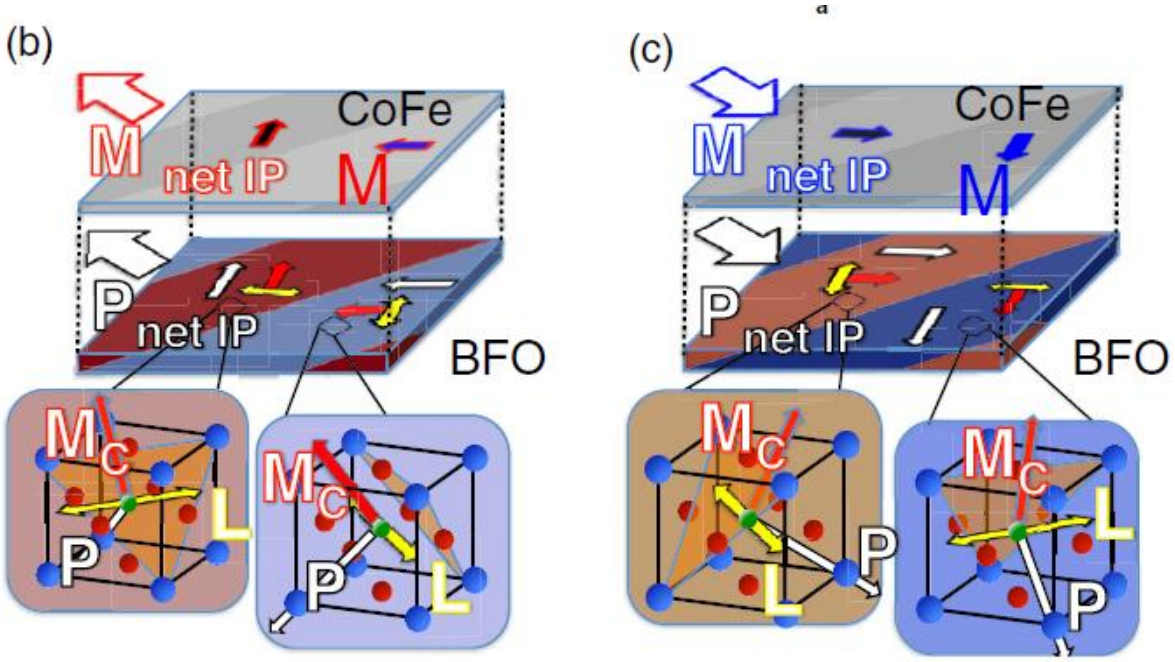

PRL **107,** 217202 (2011)

Rep. Prog. Phys. 77 (2014) 076501 (45pp)

Review Article

Multiferroics of spin origin

Yoshinori Tokura[1,2], **Shinichiro Seki**[1,3] **and Naoto Nagaosa**[1,2]

[1] RIKEN Center for Emergent Matter Science (CEMS), Wako 351-0198, Japan
[2] Department of Applied Physics, University of Tokyo, Tokyo 113-8656, Japan
[3] PRESTO, Japan Science and Technology Agency (JST), Tokyo 102-0075, Japan

Abstract

Multiferroics, compounds with both magnetic and ferroelectric orders, are believed to be a key material system to achieve cross-control between magnetism and electricity in a solid with minute energy dissipation. Such a colossal magnetoelectric (ME) effect has been an issue of keen interest for a long time in condensed matter physics as well as a most desired function in the emerging spin-related electronics. Here we begin with the basic mechanisms to realize multiferroicity or spin-driven ferroelectricity in magnetic materials, which have recently been clarified and proved both theoretically and experimentally. According to the proposed mechanisms, many families of multiferroics have been explored, found (re-discovered), and newly developed, realizing a variety of colossal ME controls. We overview versatile multiferroics from the viewpoints of their multiferroicity mechanisms and their fundamental ME characteristics on the basis of the recent advances in exploratory materials. One of the new directions in multiferroic science is the dynamical ME effect, namely the dynamical and/or fast cross-control between electric and magnetic dipoles in a solid. We argue here that the dynamics of multiferroic domain walls significantly contributes to the amplification of ME response, which has been revealed through the dielectric spectroscopy. Another related issue is the electric-dipole-active magnetic resonance, called electromagnons. The electromagnons can provide a new stage of ME optics via resonant coupling with the external electromagnetic wave (light). Finally, we give concluding remarks on multiferroics physics in the light of a broader perspective from the emergent electromagnetism in a solid as well as from the possible application toward future dissipationless electronics.

Mechanisms for electric polarization of spin origin

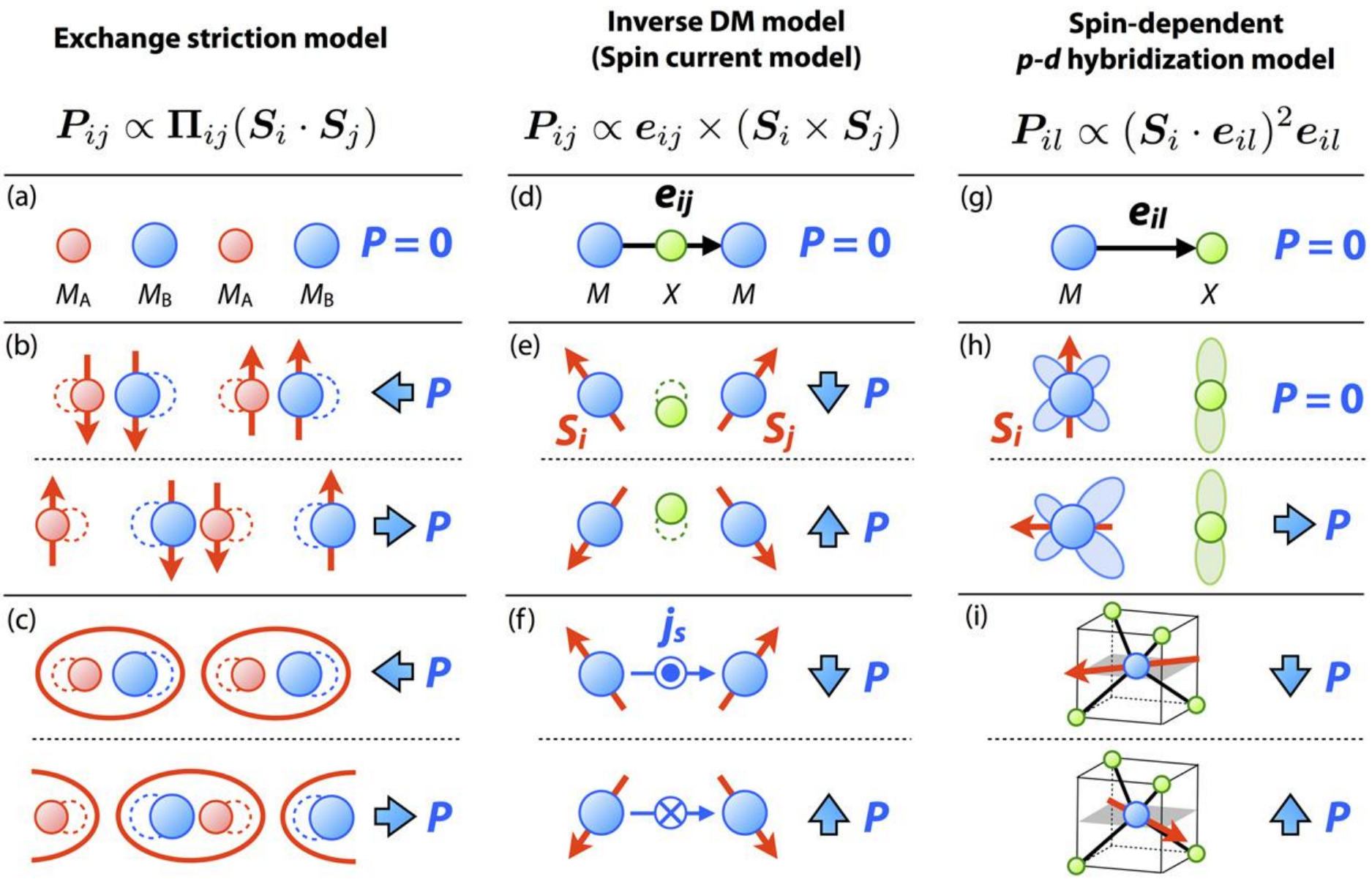

Tokura, Seki and Nagaosa: Rep. Prog. Phys. **77** (2014) 076501

Mechanisms for electric polarization of spin origin

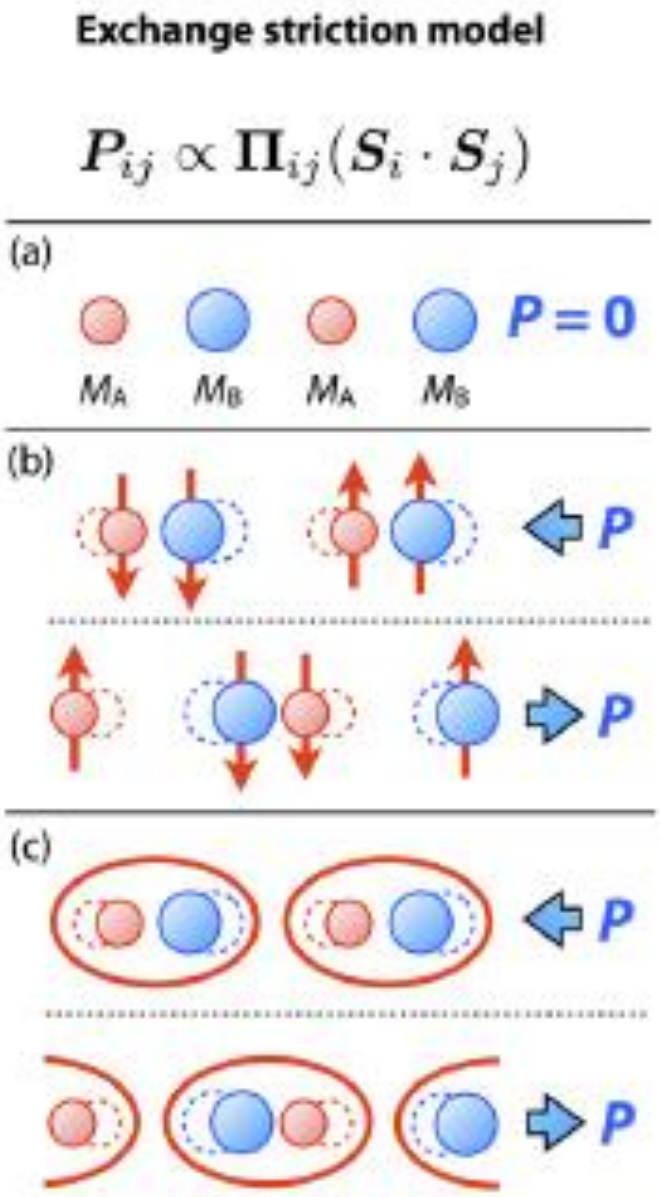

The symmetric exchange interaction working between the neighboring spins, $\boldsymbol{S}_i$ and $\boldsymbol{S}_j$, may induce striction along a specific crystallographic direction $\boldsymbol{\Pi}_{ij}$.

For ***P*** to be macroscopically produced, the spin modulation should be commensurate with the crystal lattice and the induced striction should show no cancelation after the sum of the bonds over the crystal lattice.

For example, the up–up–down–down spin arrangement along the atomically alternating A–B lattice (see (*b*)) can break the inversion symmetry, and the inequivalent exchange striction working between the up–up (or down–down) spin pair and the up–down (or down–up) one can produce ***P***.

The exchange-striction mechanism predicts the emergence of ***P*** along the bond direction for the AB lattice (i.e. alternating array of two distinctive magnetic sites M_A and M_B as shown in (*a*)), with (*b*) ↑↑↓↓ spin order or (*c*) dimer-singlet formation.

Tokura, Seki and Nagaosa: Rep. Prog. Phys. **77** (2014) 076501

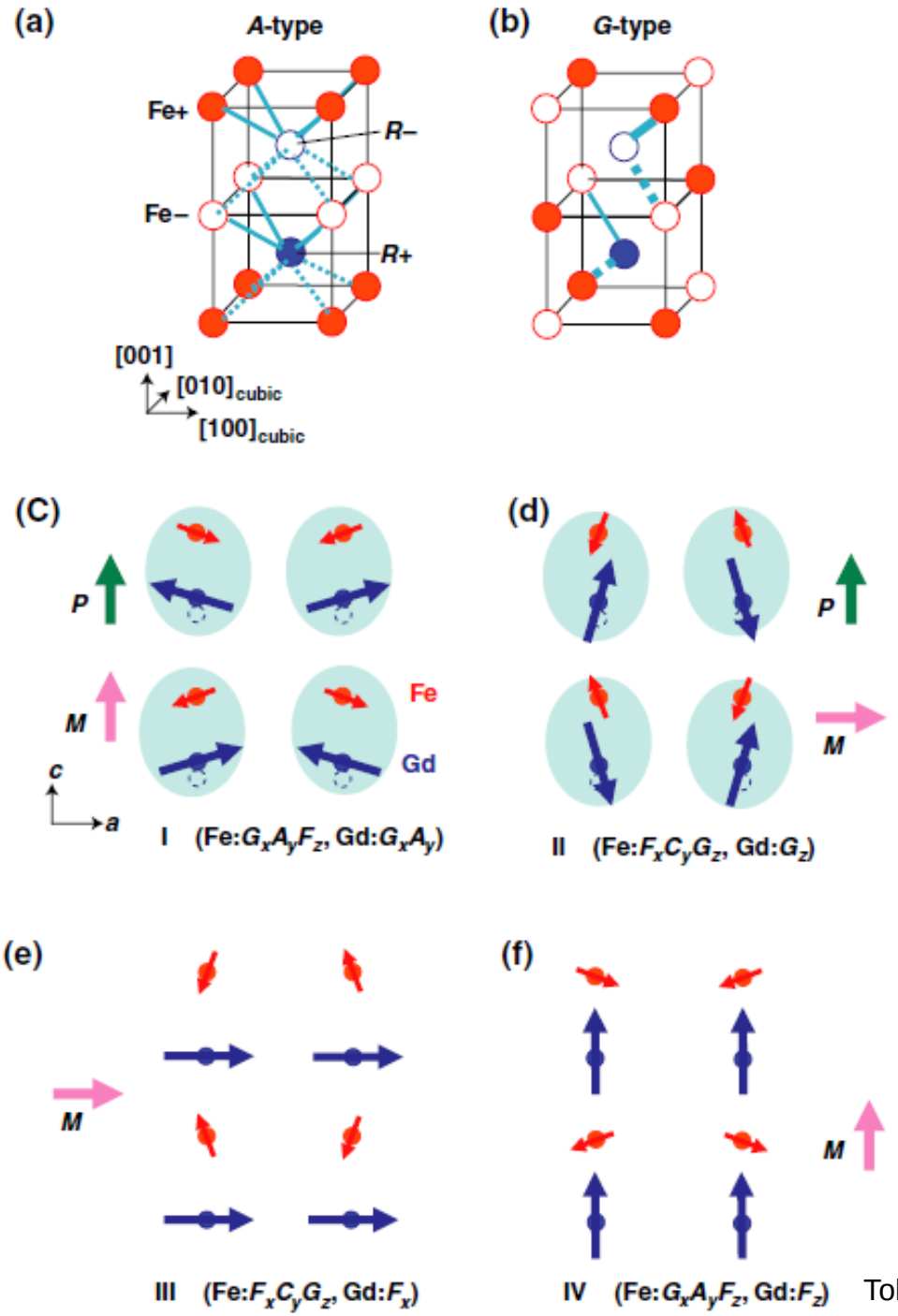

ORTOFERRITES, RFeO$_3$ (R= Gd, Tb, Dy)

Models of exchange striction in RFeO$_3$ of an orthorhombic (*Pbnm*) perovskite unit cell with the A-type (*a*) and G-type (*b*) magnetic structures. The blue solid (dotted) lines represent attractive (repulsive) interactions. The plus and minus symbols denote the relative spin direction of each ion. (*c*)–(*f*) Magnetic structures of phases I–IV shown in figure 18. Only the most strongly coupled pairs of Fe spins and Gd spins are depicted with large light blue ellipsoids. The filled blue circles represent the displaced position of Gd along the *c*-axis from its original position (open circles). Note that G, A, C, and F denote NaCl-type, layered-type, rod-type AF, and ferromagnetic components with modulation vectors *(π, π, π), (0, 0, π), (π, π, 0)*, and *(0, 0, 0)* in the cubic setting, respectively. The subscripts *x, y*, and *z* denote the directions of the components along the *a, b*, and *c* axes, respectively.

Tokura, Seki and Nagaosa: Rep. Prog. Phys. **77** (2014) 076501

Mechanisms for electric polarization of spin origin

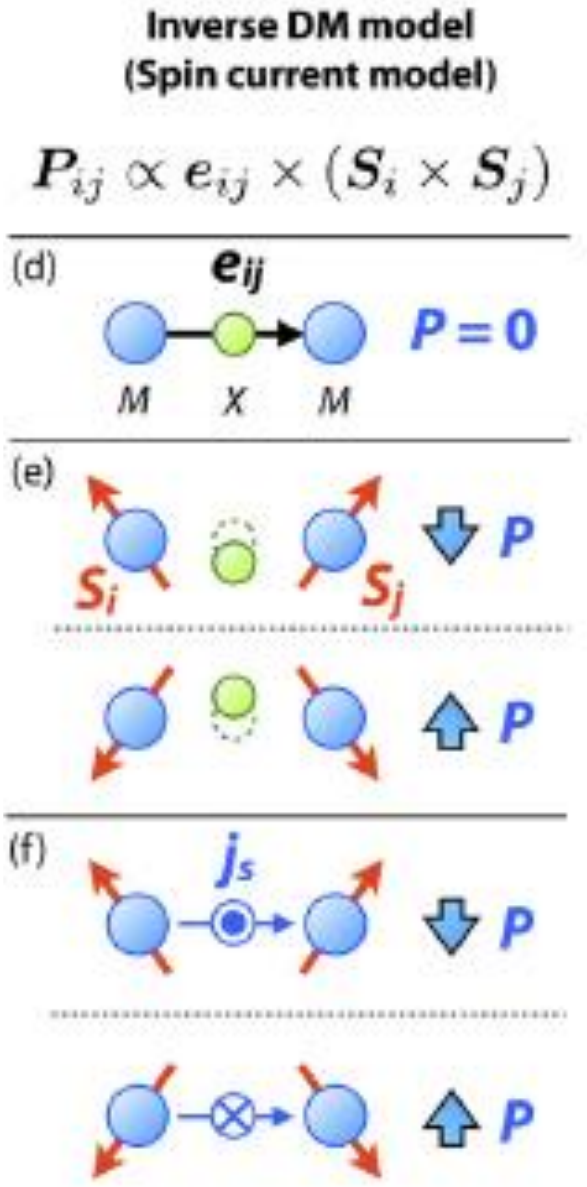

The spin current is viewed as flowing between the canted spin sites $\boldsymbol{S}_i$ and $\boldsymbol{S}_j$ (with $\boldsymbol{e}_{ij}$ being an unit vector connecting these two sites), which produces the polarization ***P*** under the influence of the spin orbit coupling (SOC) (figure (*f*)). This ***P*** can be of genuine electronic origin, yet in reality the exchange striction plays an important role in determining the magnitude of ***P***. Therefore, this term is often called the inverse Dzyaloshinskii–Moriya (DM) interaction, in which the intervening ligand atom (e.g. oxygen) can displace so as to favor the DM interaction (figure (*e*)). Such a spin-current model has been very powerful in recent exploration studies of multiferroics, since transverse screw spin configurations, such as cycloidal and transverse-conical spin orders, can always produce spontaneous ***P*** irrespective of magnetic modulation vectors, namely commensurate or incommensurate.

Tokura, Seki and Nagaosa: Rep. Prog. Phys. **77** (2014) 076501

Types of spiral magnetic structure on a chain of magnetic moments **S**(**r**)

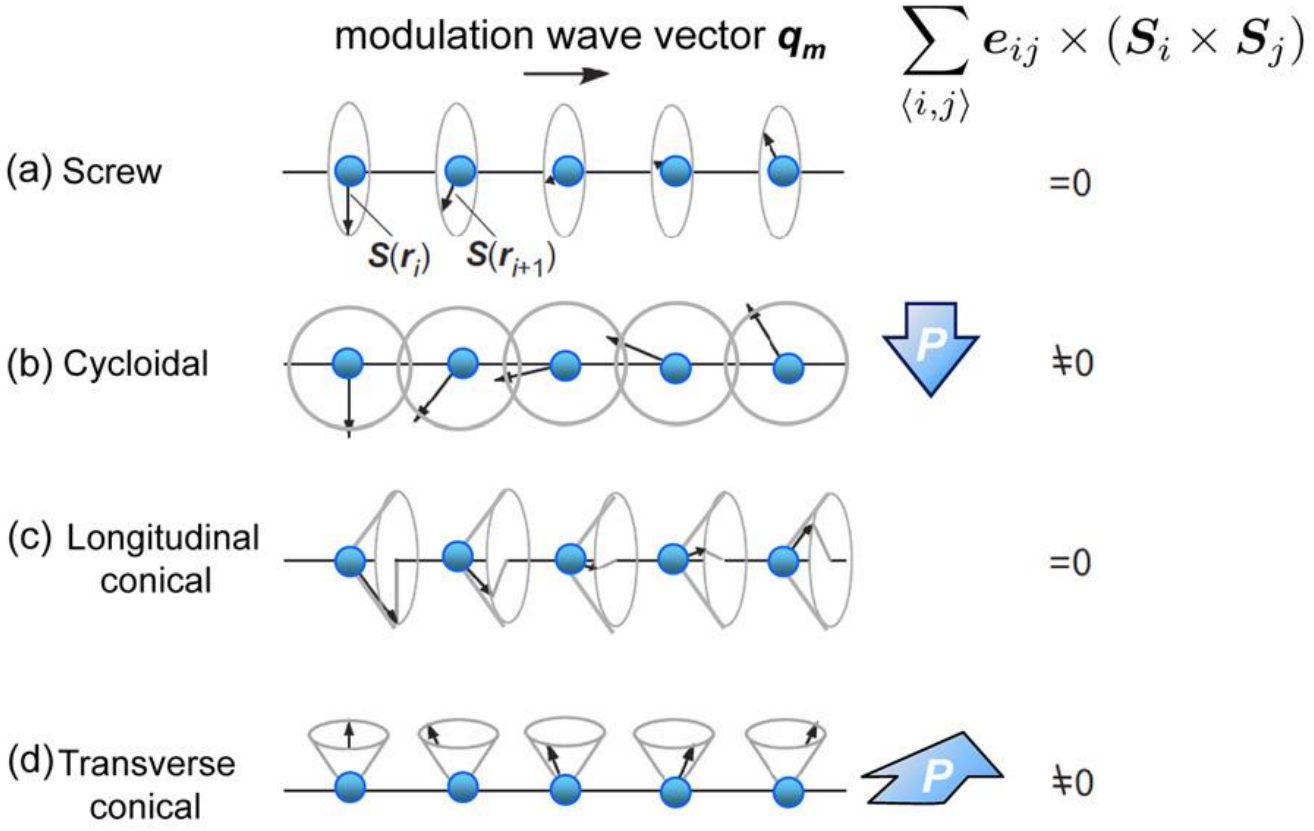

Schematic illustrations of types of spiral magnetic structure on a one-dimensional array of magnetic moments ***S****(r)*. They include (*a*) proper screw, (*b*) cycloidal, (*c*) longitudinal-conical, and (*d*) transverse-conical magnetic structures. The directions of macroscopic polarization ***P*** calculated from the spin-current model or inverse DM model are also indicated for their respective structure. Other spiral structures (*a*) and (*c*) may potentially generate ***P*** due to the spin-dependent *p*–*d* hybridization mechanism on some specific crystal structures.

Tokura, Seki and Nagaosa: Rep. Prog. Phys. **77** (2014) 076501

Perovskite manganites

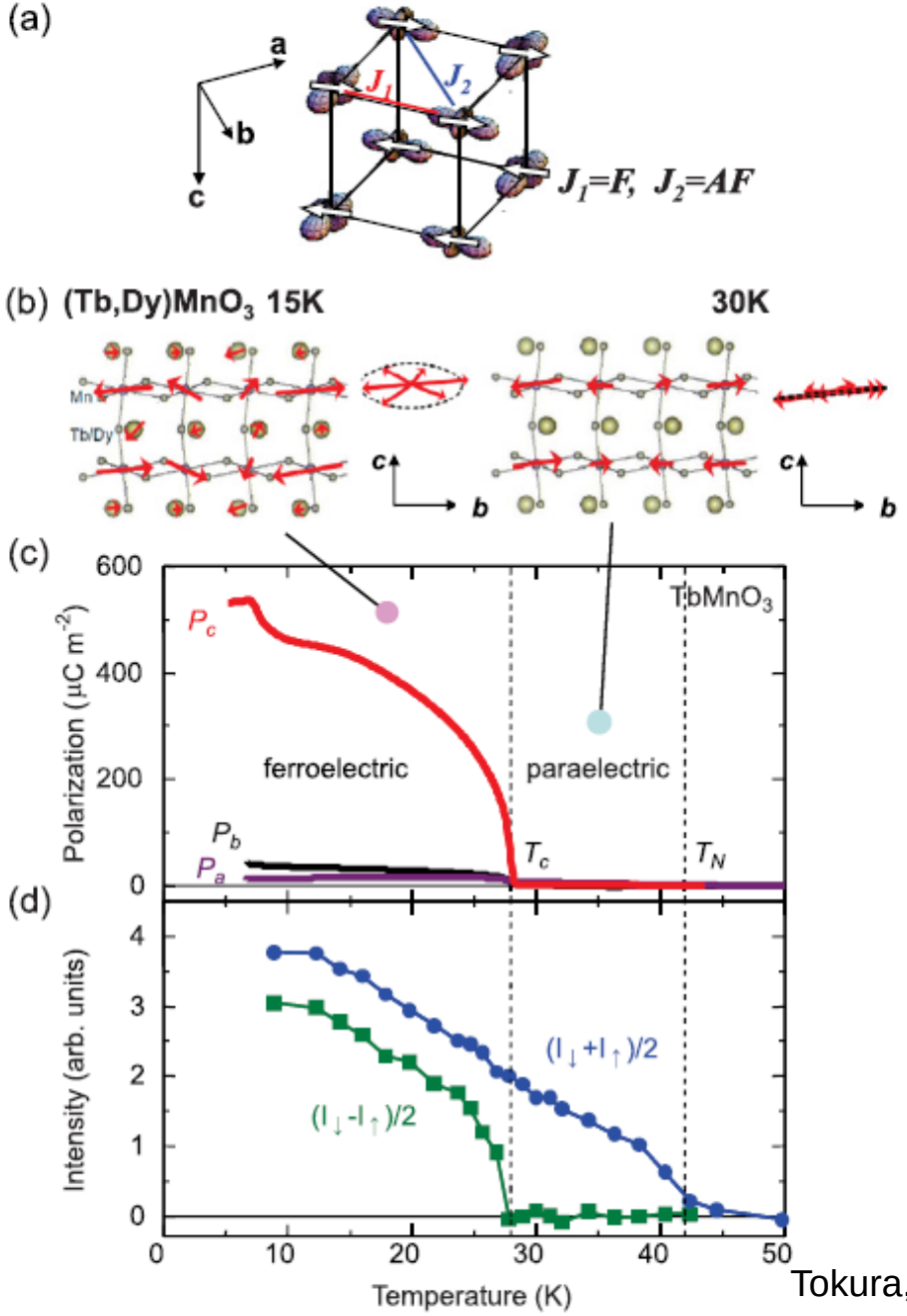

(*a*) Schematic illustration of spin/orbital ordered state and magnetic exchange interactions for $LaMnO_3$. (*b*) The solved magnetic structures at Mn sites in the paraelectric AF phase ($T_c < T < T_N$) and FE AF phase ($T < T_c$) for (Tb, Dy)MnO_3 ($q_m = 1/3$). (*c*) Temperature profiles of electric polarization along the *a*, *b*, and *c* axes for $TbMnO_3$. (*d*) The corresponding temperature dependence of the polarized neutron scattering intensity at $Q = (4, +q_m, 1)$. $I_\downarrow$ and $I_\uparrow$ indicate the scattering intensities for the neutron spin parallel and antiparallel to *Q*, respectively.

Tokura, Seki and Nagaosa: Rep. Prog. Phys. **77** (2014) 076501

Mechanisms for electric polarization of spin origin

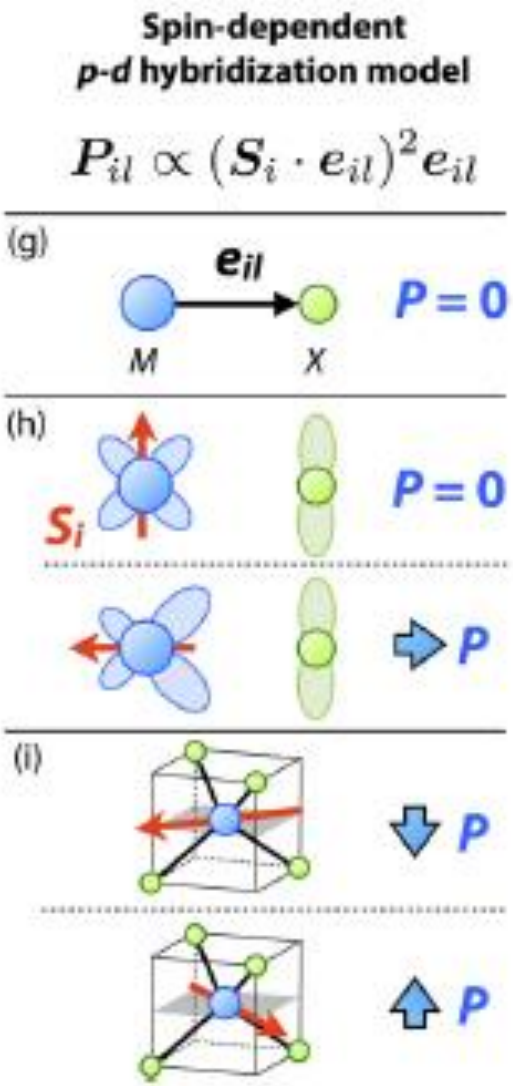

The spin-dependent p–d hybridization mechanism is based on the fact that the locally polar bond ***e**il* connecting the spin site *i* and the ligand site *l* can be modulated by the spin-direction dependent hybridization arising from the SOC (figure (*h*)). When the sum over the crystal lattice sites is not cancelled, the macroscopic ***P*** can survive. The spin-dependent p–d hybridization model considers (*g*) a single pair of *M* and *X* sites, and local ***P*** is induced along the bond direction due to (*h*) the spin-dependent modulation of covalency between the magnetic d orbital and ligand p orbital.

With some appropriate crystallographic lattice such as (*i*) MX_4 tetrahedra, this term can avoid cancellation and cause macroscopic ***P***.

Spin-dependent p–d hybridization mechanism does need both SOC and specific lattice form, but can occur irrespective of commensurate or incommensurate order. Thus, we can sometimes identify which mechanism is working for the emergence of multiferroicity in the material by knowing the crystal and magnetic structure precisely.

It is to be noted that two of these mechanisms can coexist in actual multiferroics.

Tokura, Seki and Nagaosa: Rep. Prog. Phys. **77** (2014) 076501

Table 2. List of multiferroic compounds with magnetically induced ferroelectricity.

Mechanism	Magnetic order	Compound	Ref.
Spin current	Cycloidal	$RMnO_3$ (R = Tb, Dy, ...)	[34]
		$Ni_3V_2O_8$	[52]
		$MnWO_4$	[49, 53]
		$LiCu_2O_2$	[50, 54]
		$LiCuVO_4$	[56, 57]
		$CuCl_2$, $CuBr_2$	[58, 60]
		CuO	[51]
	(H-induced) Conical	$CoCr_2O_4$	[61]
		$ZnCr_2Se_4$	[62]
		$Ba_{0.5}Sr_{1.5}Zn_2Fe_{12}O_{22}$	[63]
		$Ba_2Mg_2Fe_{12}O_{22}$ (BMFO)	[64]
Exchange striction	Collinear antiferromagnetic	RMn_2O_5 (R = Tb, Dy, ...)	[65]
		Ca_3CoMnO_6	[66]
	Weak ferromagnetic	$DyFeO_3$, $GdFeO_3$	[67, 68]
	Spin singlet	TTF-bromanil	[69]
	Collinear incommensurate	$FeTe_2O_5Br$	[70]
	Noncollinear ferrimagnetic	$CaBaCo_4O_7$	[71, 72]
p–d hybridization	Proper screw	$CuFeO_2$	[73]
		MnI_2, NiI_2	[74, 75]
	120°	$CuCrO_2$, $AgCrO_2$	[76]
		$RbFe(MoO_4)_2$	[77]
	Collinear antiferromagnetic	$Ba_2MGe_2O_7$ (M = Co, Mn)	[78–80]
		CuB_2O_4	[81]
		$RFe_3(BO_3)_4$	[82, 83]
	Skyrmion	Cu_2OSeO_3	[84, 85]

Tokura, Seki and Nagaosa: Rep. Prog. Phys. **77** (2014) 076501